RADIANT ENERGY EXCHANGE ABOVE AND WITHIN A DWARF APPLE ORCHARD

RADIANT ENERGY EXCHANGE ABOVE AND WITHIN A DWARF APPLE ORCHARD

by

PHILIP WAYNE SUCKLING, B.Sc.

A Thesis

Submitted to the Faculty of Graduate Studies

In Partial Fulfilment of the Requirements

for the Degree

Master of Science

McMaster University

May 1974

MASTER OF SCIENCE (1974)
(Geography)

McMASTER UNIVERSITY
Hamilton, Ontario

TITLE: Radiant Energy Exchange Above and Within a Dwarf Apple Orchard

AUTHOR: Philip Wayne Suckling, B.Sc. (McMaster University)

SUPERVISOR: Professor J.A. Davies

NUMBER OF PAGES: xi, 78

SCOPE AND CONTENTS:

The radiation balance of a dwarf apple orchard was evaluated. Results compared favourably with those for a single apple tree in an earlier investigation. Reflection, heating and longwave exchange coefficients were analysed.

Transmitted global radiation was measured with moving and stationary sensors. Coefficients for the partitioning of incident global radiation were calculated. A relationship between photosynthetically active radiation and global radiation was established. Coefficients for the partitioning of incident photosynthetically active radiation were obtained and compared to the global radiation components. A problem associated with the measurement of transmitted radiation is discussed briefly.

ACKNOWLEDGEMENTS

I wish to thank my supervisor, Dr. J.A. Davies for his guidance and assistance throughout this study. Also, I acknowledge the advice and comments of the other members and students of the Department of Geography.

I am especially grateful to Dr. J.T.A. Proctor of the Horticultural Experiment Station, Simcoe, Ontario for his help and advice during my field work, and for supplying instrumentation. I would also like to thank Dr. G. Collin and the other staff members at the Station for their assistance.

This study was supported, in part, by the National Research Council of Canada.

TABLE OF CONTENTS

LIST OF PLATES

LIST OF TABLES

LIST OF FIGURES

LIST OF SYMBOLS

Symbol	Explanation	Units
D	diffuse radiation	Wm^{-2}
$K\downarrow$	incoming global radiation	Wm^{-2}
$K\uparrow$	reflected global radiation	Wm^{-2}
K^*	net global radiation	Wm^{-2}
K_A	absorbed global radiation	Wm^{-2}
K_T	transmitted global radiation	Wm^{-2}
$K_p\downarrow$	incoming PAR	Wm^{-2}
$K_p\uparrow$	reflected PAR	Wm^{-2}
K_{pA}	absorbed PAR	Wm^{-2}
K_{pT}	transmitted PAR	Wm^{-2}
LAI	leaf area index	m^2m^{-2}
$L\downarrow$	incoming longwave atmospheric radiation	Wm^{-2}
$L\uparrow$	upward or emitted terrestrial radiation	Wm^{-2}
L^*	net terrestrial radiation	Wm^{-2}
$L^*(0)$	net terrestrial radiation when $K^* = 0$	Wm^{-2}
NIR	near infra-red radiation	
PAR	photosynthetically active radiation	
$Q\downarrow$	incoming total radiation	Wm^{-2}
Q^*	net radiation	Wm^{-2}
r	linear correlation coefficient	*dimensionless*
Z	solar zenith angle	*deg*
α	reflection coefficient or albedo	*dimensionless*

$\bar{\alpha}$	mean daily reflection coefficient	*dimensionless*
α_p	PAR reflection coefficient	*dimensionless*
$\bar{\alpha}_p$	mean daily PAR reflection coefficient	*dimensionless*
β	heating coefficient	*dimensionless*
δ	ratio of $D/K\downarrow$	*dimensionless*
$\bar{\delta}$	mean daily ratio of $D/K\downarrow$	*dimensionless*
λ	longwave exchange coefficient	*dimensionless*
$\emptyset$	absorption coefficient	*dimensionless*
$\bar{\emptyset}_p$	mean daily absorption coefficient	*dimensionless*
$\emptyset_p$	PAR absorption coefficient	*dimensionless*
$\bar{\emptyset}_p$	mean daily PAR absorption coefficient	*dimensionless*
τ	transmission coefficient	*dimensionless*
$\bar{\tau}$	mean daily transmission coefficient	*dimensionless*
τ_p	PAR transmission coefficient	*dimensionless*
$\bar{\tau}_p$	mean daily PAR transmission coefficient	*dimensionless*

CHAPTER I

INTRODUCTION

1. Radiation in an apple orchard

An important factor in controlling the productivity of agricultural crops is the intensity and spectral distribution of the radiant energy received. This energy is used for the physiological process of photosynthesis, and determines the microclimate of the crop, thus influencing environmental factors such as the moisture regime, ecological competition, presence of parasites, and plant disease, all of which effect crop yield. Hence, radiant energy properties above and within plant canopies have direct and indirect influences on crop productivity.

The radiation balance of a crop can be expressed as

$$Q^* = K^* + L^* = K\downarrow - K\uparrow + L\downarrow - L\uparrow, \tag{1}$$

where Q^* is net radiation, K^* is net global radiation, L^* is net terrestrial radiation, $K\downarrow$ is incoming global radiation, $K\uparrow$ is reflected global radiation, $L\downarrow$ is incoming longwave atmospheric radiation and $L\uparrow$ is outgoing or emitted terrestrial radiation. Global radiation is the energy received within the *0.4 to 4.0* μm waveband of the electromagnetic spectrum, while terrestrial or longwave radiation is the energy at wavelengths greater than *4* μm (Sellers, 1965). Incoming global radiation has two components: direct beam solar radiation and diffuse radiation.

From equation *1*, $K^* = K{\downarrow}\,(1-\alpha)$ where α is the surface reflection coefficient defined as $K{\uparrow}/K{\downarrow}$. Proctor, Kyle and Davies (1972) have studied the radiation balance terms for a single, full-sized apple tree. Extension of their work to a complete apple tree orchard canopy is a logical development.

Although the balance is influenced by surface control exerted through $K{\uparrow}$ and $L{\uparrow}$, it is dominated by the incoming fluxes of global and longwave radiation. If these can be calculated successfully, the balance may be estimated without resort to measurement. This reduces the cost and complexity of maintaining sophisticated sensing and recording instrumentation. Hence, development and testing of radiation models is an important test.

A knowledge of the radiation balance at the upper orchard boundary is needed to compare and evaluate energy exchange parameters within the canopy. The transmission of global radiation into the orchard is important in determining the maximum density of trees that can be maintained successfully without depleting the irradiance of lower leaves detrimentally. The global radiation in the *0.4* to *0.7* μm waveband, which drives the plant photosynthetic system, will be referred to as the photosynthetically active radiation. The behaviour of PAR within a canopy is important in the understanding of productivity.

2. Objectives of the study

The radiant energy exchanges above and within an experimental, high density planting of dwarf apple trees are investigated. The specific aims of the study are:

1. to determine the radiation balance and its components

above the orchard and to test radiation balance models, and

2. to evaluate canopy transmission, reflection and absorption coefficients for global and photosynthetically active radiation.

This information may assist in determining optimum yields from such planting schemes with this species.

CHAPTER II

SITE AND INSTRUMENTATION

1. Research site

The study was conducted at the Horticultural Experiment Station of the Ontario Ministry of Agriculture and Food near Simcoe, Ontario (42° 51' N, 80° 16' W) during the summer of 1973. The orchard consisted of a 6 x 22 m plot of Malus pumila Mill. cultivar Idared (Rehder, 1962) on a dwarf tree stock (*Plate 1*). The trees were arranged in 5 rows of 15 trees each, with both trees and rows spaced about 1.5 m apart. Successive rows were staggered (*Figure 1*). The trees were approximately 2 m tall in mid-June and had reached a height of 2.5 m by September. Leaf area index (LAI) was measured only once, on September 14, after some leaves had begun to fall due to dry weather in late August and early September. The LAI was determined by establishing a correlation between leaf area and leaf weight from a random sample of leaves (Chang, 1968). Estimated from leaf weight, LAI was 0.945.

2. Instrumentation

A complete radiation balance of the orchard was obtained by measuring incoming global radiation $K\downarrow$, incoming total radiation $Q\downarrow$, diffuse radiation D, reflected global radiation $K\uparrow$, and net radiation Q^*. The reflection coefficient was calculated and the incoming atmospheric radiation was found from

PLATE 1: THE DWARF APPLE ORCHARD

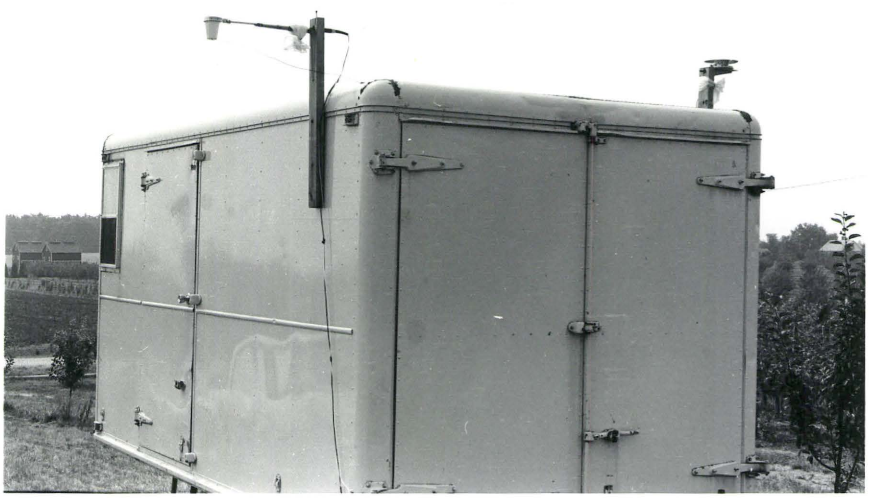

PLATE 2: RECORDING TRAILER WITH INCOMING GLOBAL AND TOTAL RADIATION SENSORS

Figure 1: THE APPLE ORCHARD AND LOCATION OF SENSORS

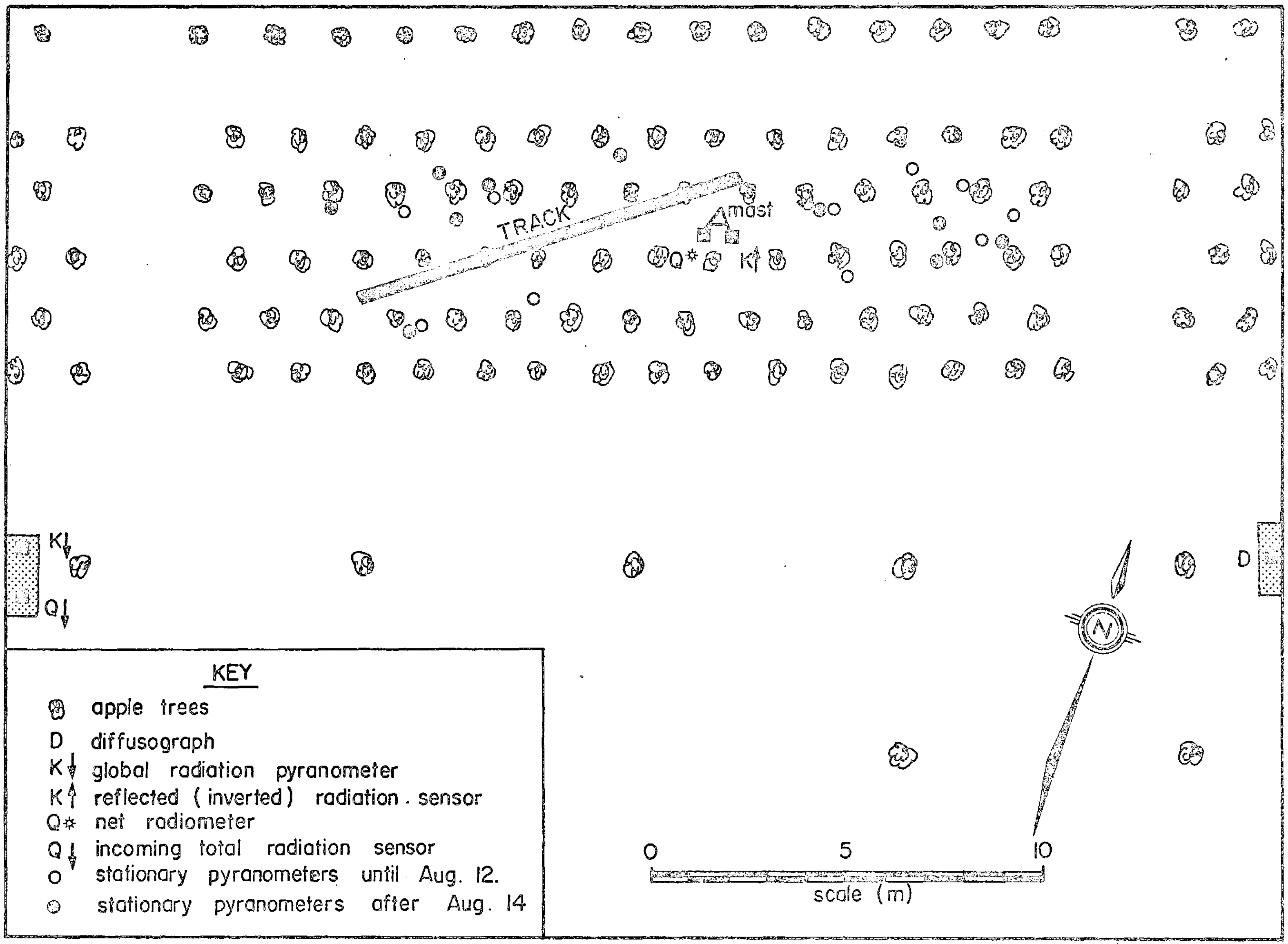

$$L\downarrow = Q\downarrow - K\downarrow. \tag{2}$$

Upward terrestrial radiation $L\uparrow$ was determined as a residual from *equation 1*.

Global radiation was measured with a precision pyranometer (Eppley Laboratory Inc., Newport, R.I., USA) and incoming total radiation with a net radiometer (Model S1, Swissteco Pty. Ltd., Melbourne, Australia) fitted with a black-body adaptor to shield the sensor from $L\uparrow$. The adaptor temperature (T_c) was measured with a thermocouple referenced to an ice-point temperature (Icell reference temperature unit, Thermo Electric, Brampton, Ontario). $Q\downarrow$ was calculated from

$$Q\downarrow = Q\downarrow' + \sigma T_c^4, \tag{3}$$

where $Q\downarrow'$ is the radiometer signal divided by the sensor calibration factor and σ is the Stefan-Boltzman constant. Both radiometers were mounted on the roof of the recording trailer *(Plate 2)*. Incoming diffuse radiation was measured using a pyranometer (Kipp and Zonen, Delft, The Netherlands) mounted within an Atmospheric Environment Service diffusograph *(Plate 3)* set on the roof of a small hut near the orchard. Reflected global radiation was measured with a similar pyranometer while net radiation was obtained from a Swissteco net radiometer. Both of these were mounted on a mast in the orchard *(Plate 4)*. To assure that the field of view of the instruments was confined to the orchard, instruments were located at a height of 3 m, about 0.5 m above the tops of the trees. This resulted in a view factor of about 0.96 (Latimer, 1972).

PLATE 3: THE DIFFUSOGRAPH

PLATE 4: NET RADIOMETER AND INVERTED PYRANOMETER

Recently, transmitted radiation has been measured using moving sensors by several researchers (Rodskjer and Kornher, 1971; Mukammal, 1971; Brown, 1973). A traversing system was designed to transport precision Eppley pyranometers through the orchard beneath the foliage. Tracks were made of Dexion metal strips supported by adjustable pipes and flanges. The two tracks, 9.5 m long and 0.31 m apart, traversed the rows of trees at a 20° angle (*Figure 1*). The track was set at a height of about 0.35 m above the ground and levelled. A motor and pulley drew a plexiglass cart *(Plates 5 and 6)* carrying the sensors along the track at a speed of approximately 1.9 m/min. Microswitches at each end of the track reversed the direction of the motor resulting in one round trip every ten minutes. Two precision pyranometers were mounted on the cart (*Plate 5*). One measured global radiation while the second, fitted with a dome of RG8 glass measured the near infra-red radiation (NIR) of wavelength greater than 0.7 μm (*Figure 2*). The difference between the two measurements is PAR. The RG8 filter has been used successfully by several researchers (Szeicz, 1966, 1970; Anderson, 1969; Rodskjer, 1971). Since only one pyranometer with an RG8 dome was available, it was placed in the open to monitor incoming NIR on selected days in order to establish a relationship between incident PAR and global radiation.

A grid of ten stationary pyranometers was established in the canopy. The results from these stationary sensors could be compared with the results from the traversing sensor. Four black and white Eppley pyranometers, two Kipp pyranometers and four Swissteco radiometers fitted with glass domes were randomly located within the orchard (*Figure 1*)

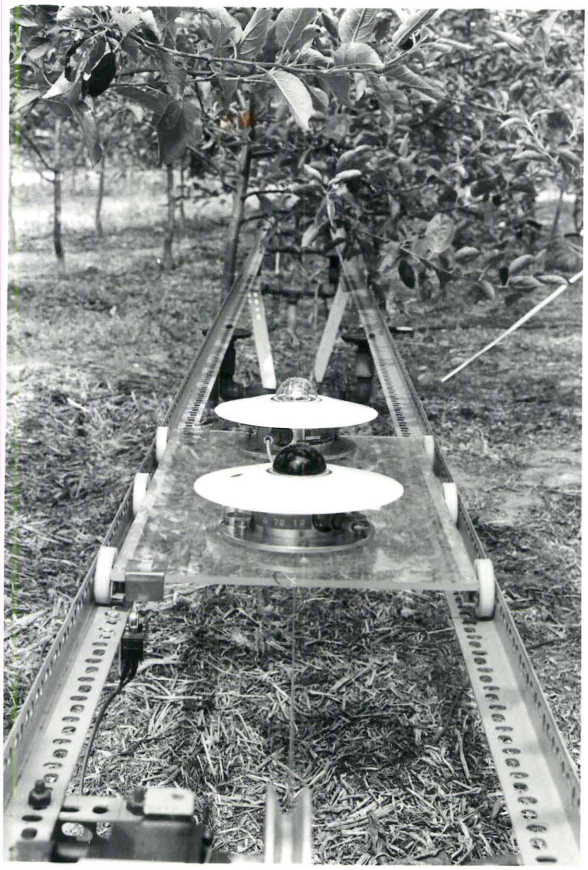

PLATE 5: THE TRAVERSING CART AND TRACK SYSTEM

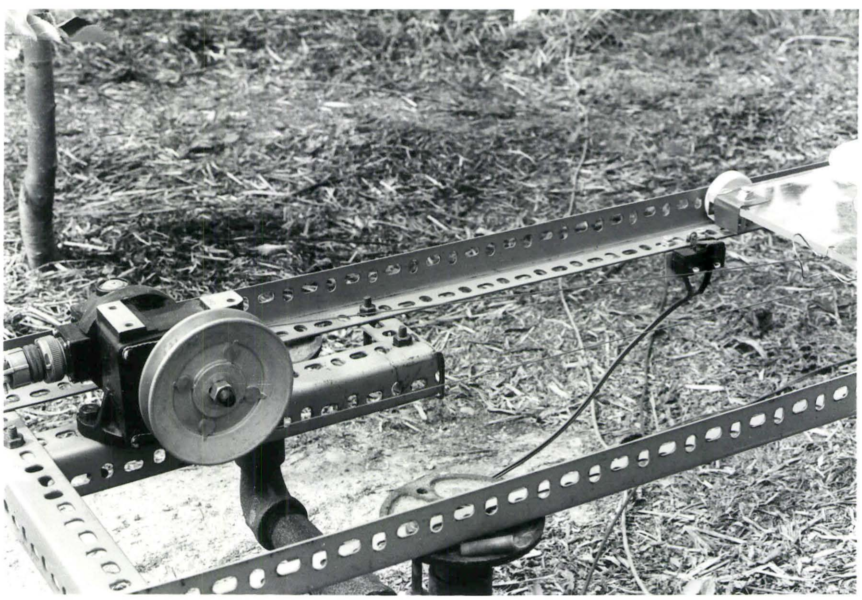

PLATE 6: MOTOR, PULLEY AND MICROSWITCH OF TRAVERSING SYSTEM

Figure 2: TRANSMITTANCE OF THE SCHOTT RG8 FILTER

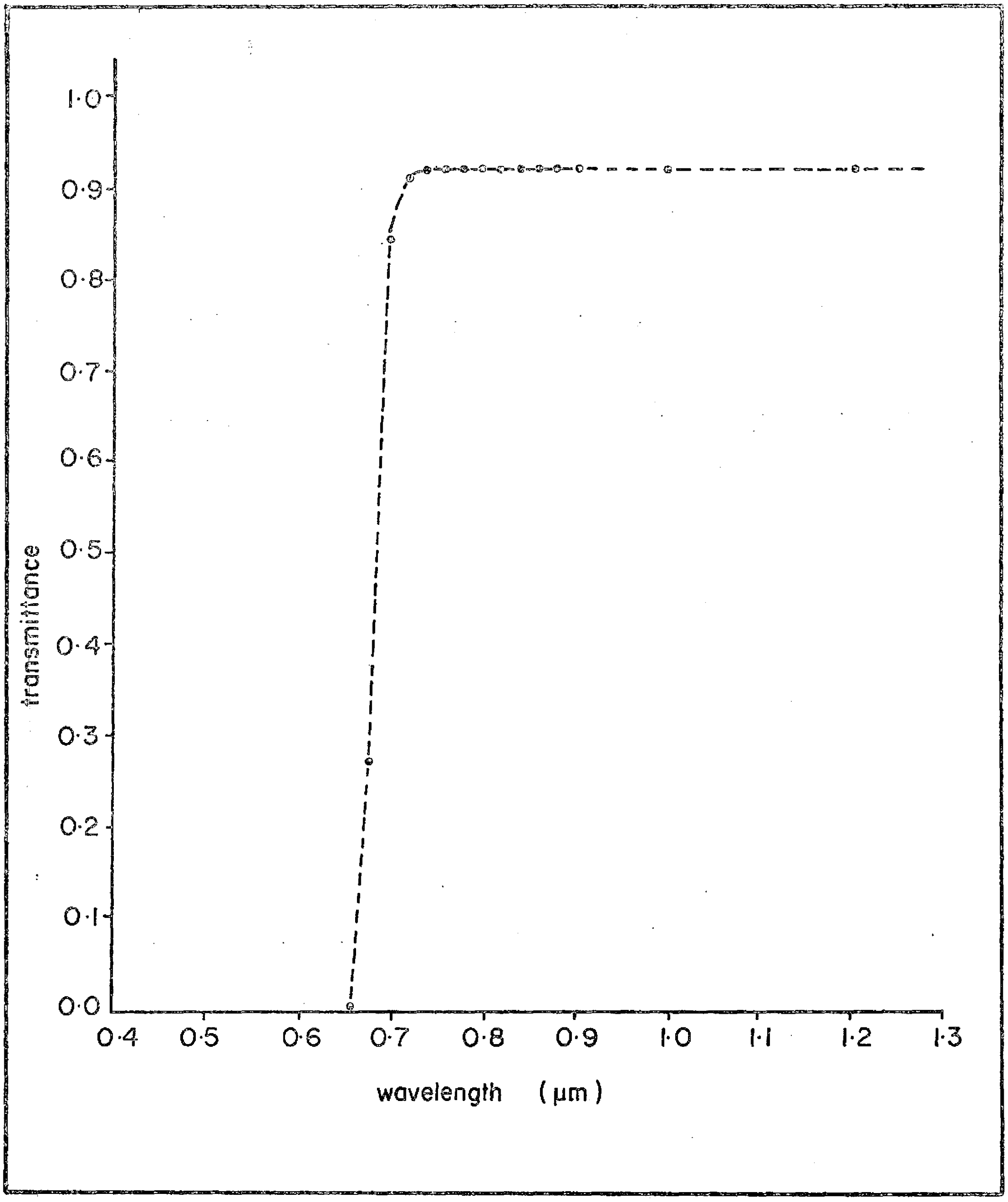

at a height above the ground corresponding to the height of the instruments on the traversing system. Measurements were taken at the same time as those from the moving sensors. The stationary sensor grid was relocated on August 14 to allow the results of two different random locations to be compared.

The calibrations provided by the manufacturers for the Swissteco and precision Eppley sensors were accepted. The two precision Eppley pyranometers with clear glass domes were nevertheless compared on several days under cloudless skies, yielding results that varied by less than 2% at all times. The Kipp and black and white Eppley pyranometers were calibrated under cloudless skies against the precision Eppley pyranometers on July 16 and 17. The Kipp pyranometers agreed well with calibrations given by the manufacturers whereas slight deviations from the original calibrations were found for the Eppleys. These latter sensors were several years old whereas all other sensors were new or only one year old. The Eppleys suffered from paint peeling late in August; hence, no results from these sensors were accepted after August 15.

All signals from the radiation sensors were led to the recording trailer by means of shielded cables to minimize external electrical noise. Signals were recorded on three multipoint recorders (Esterline Angus Division, Esterline Corp., Indianapolis, Indiana). Shortwave radiation signals of $K\downarrow$, $K\uparrow$, and D, the ice-point reference signal for $Q\downarrow$, and the signals from the ten stationary pyranometers within the canopy were recorded on one recorder. A second recorder was used for the signals from the traversing sensors. Net radiation and the signal from the incoming total radiation sensor were recorded on the third Esterline-Angus recorder. The signals were received once every 10 seconds for the first recorder (once every 25 seconds when the stationary pyranometers were in operation), once every 4 seconds for the second, and once every 30 seconds for the third recorder. Data from the charts were extracted by hand scaling.

3. Operating procedure

On a typical operating day, radiation sensors and the track were wiped clean and checked for levelling and smoothness of operation in the morning. The ice-point reference unit, nitrogen flow for the net and incoming total radiometers and the zero point on the multipoint recorders were checked. The radiation balance sensors were started at 0615 and run until 1745. Half-hourly values of the various terms were obtained. During the shorter days of September, the operation was curtailed by one hour at the ends of the day. The traversing system was operated once every hour for ten minute periods (corresponding to one round-trip of the cart). Stationary pyranometers within the orchard were recorded for the same periods. At the end of the day, sensors were protected with plastic bags and the recorders reset for the next day.

Measurements of incident PAR were taken on several selected days by placing the cart from the traversing system in the open on a levelled table. Care was taken to ensure that the cart was located to minimize horizon obstruction. Calibrations of some of the radiometers mentioned previously were made on July 16 and 17 in a similar manner.

Table 1 summarizes the dates when measurements were obtained. 'Cloudless' and 'cloudy' refer to days that were almost entirely under these steady-state conditions. Cloudy-bright conditions, which occur under cumulus clouds, were avoided since canopy produced variations are of central interest in this study. Since cumulus clouds associated with breezes from Lake Erie are common at Simcoe during the summer, the number of days with satisfactory data is limited.

TABLE 1

SUMMARY OF DAYS WHEN DATA WERE OBTAINED

date	radiation balance terms		transmitted radn. (moving sensor)		transmitted radn. (stationary)		incident PAR	
	Cs	Cly	Cs	Cly	Cs	Cly	Cs	Cly
June 11	X		X				X	
June 14							X	
June 19		X		X				
June 25	X		X					
June 26		X		X		X		
July 3		X						
July 9	X		X		X			
July 12							X	
July 16							X	
July 17							X	
July 18							X	
July 23	X		X					
July 30		X						
Aug. 7		X		X		X		
Aug. 12	X		X		X			
Aug. 13							X	
Aug. 14		X		X		X*		X
Aug. 15	X		X		X*			
Aug. 27		X		X				
Sept.4	X		X					
Sept.11	X							
Sept.18							X	

(Cs = cloudless; Cly = cloudy days)
(* refers to second stationary sensor grid)

CHAPTER III

RADIATION BALANCE OF A DWARF APPLE ORCHARD

1. Incoming global and longwave radiation

Many models have been proposed to estimate $K\downarrow$ and $L\downarrow$, but in this study, only two will be considered. They were selected on the basis of previous experience in the Geography Department at McMaster University which showed them to be superior (Nunez, Davies and Robinson, 1971; Robinson, Davies and Nunez, 1972). To avoid complexity introduced by cloud, only cloudless skies will be tested. The models of Houghton (1954) for $K\downarrow$ and Swinbank (1963) for $L\downarrow$ will be used.

Values of $K\downarrow$ and $L\downarrow$ were obtained for half-hourly, hourly and daily periods. Global radiation on selected cloudless days was compared to values calculated from a model based on Houghton's (1954) work

$$K\downarrow = I_o \cos Z[\phi_{wa}\,\phi_{da}\,\phi_{ws}\,\phi_{RS}\,\phi_{ds} + \tfrac{1}{2}(\phi_{wa}\,\phi_{ds}\,(1-\phi_{ws}\,\phi_{RS}\,\phi_{ds}))] \tag{4}$$

where I_o is the solar constant, ϕ_{wa}, ϕ_{da}, ϕ_{ws}, ϕ_{RS}, ϕ_{ds} are specified transmissions for water vapour absorption, dust absorption, water vapour scattering, Rayleigh scattering and dust scattering. These are expressed as functions of either the air mass number or the product of this number and precipitable water (the latter in the case of ϕ_{wa} and ϕ_{ws}). Precipitable water was calculated from radiosonde ascent data for Buffalo International Airport. Model values were computed for each hour and integrated for the day. Model and measured values compared favourably except on July 23, a hazy day, when model values overestimated *(Figure 3)*. On a daily basis *(Table 2a)*, model values were generally within 10% of the measured. If one day, July 23, is excluded, agreement is within 6%. Hence, in cloudless conditions, it seems likely that the model can replace direct measurements.

Swinbank's (1963) empirical relationship for estimating $L\downarrow$ under cloudless skies is

$$L\downarrow = (53.1)\, 10^{-14}\, T^{6}, \qquad (5)$$

where T is air (screen - level) temperature in degrees Kelvin. Considerable deviation was found between measured and calculated hourly values for five cloudless days *(Figure 4)* with peak overestimations by Swinbank's equation occurring during midday. Hourly residuals (measured - model), tabulated in *Table 2c*, show a systematic variation as found by Paltridge (1970a). Daily totals *(Table 2b)* indicate a consistent over-estimation of $L\downarrow$ by the equation. From Paltridge's data, daytime over-estimation may be balanced by underestimations at night resulting in accurate daily totals. Although nocturnal measurements were not available in the present study, the positive deviation at 0730 indicates that this may be true. Over 24 hours, the Swinbank formula probably provides satisfactory results. On an hourly basis, a variable correction has to be applied. Although Paltridge (1970a) used the mean residual curve for this to arrive at seasonal mean fluxes, this approach is not suitable for individual days. A further study which seeks to relate the residual to other factors is required.

Figure 3 : MEASURED AND CALCULATED K↓ ON CLOUDLESS DAYS

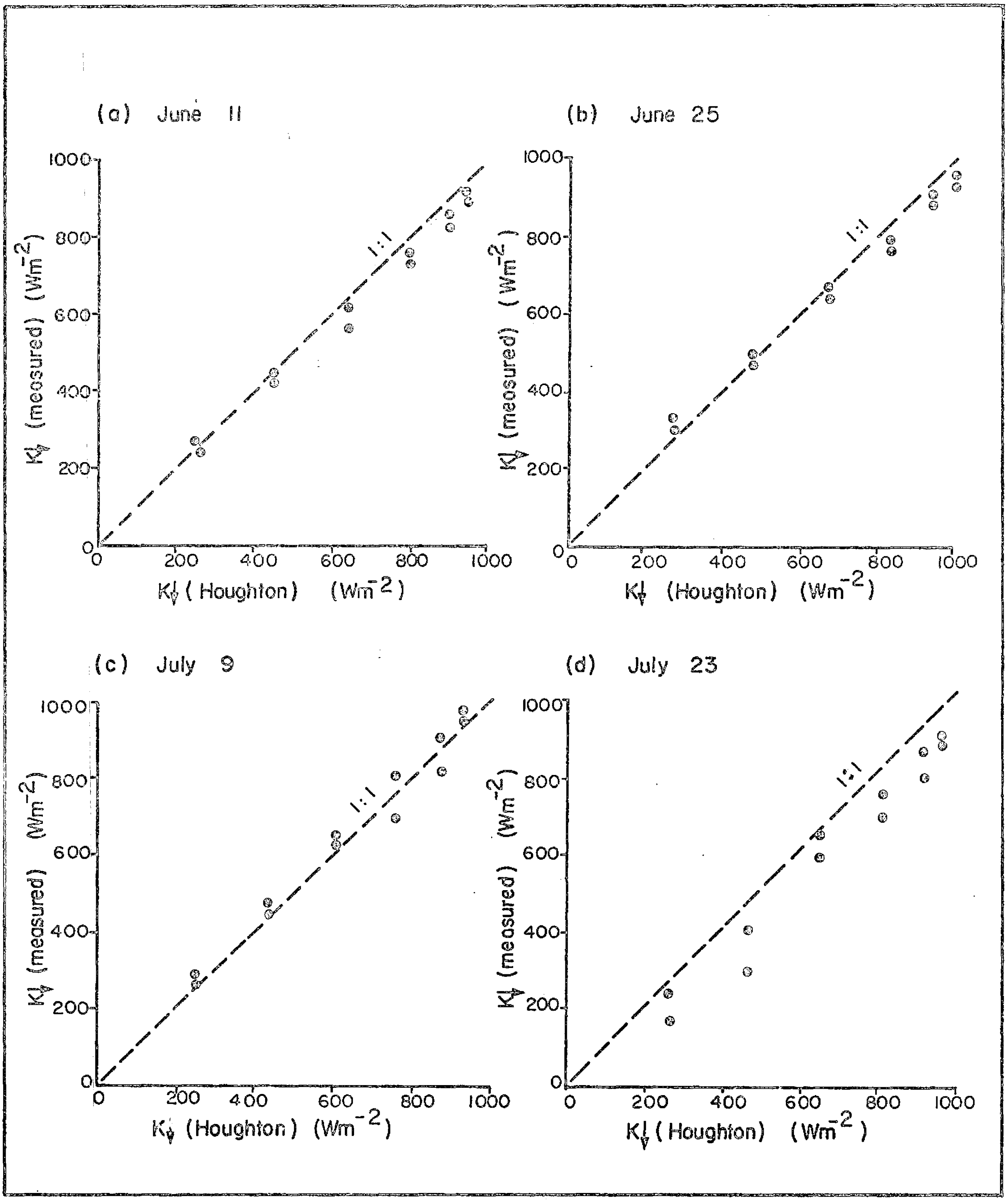

TABLE 2

INCOMING RADIATION FOR CLOUDLESS DAYS

(a) Daily totals of $K\downarrow$ measured and calculated by Houghton's (1954) model.

date	$K\downarrow$(meas) ($Kwh\ m^{-2}$)	$K\downarrow$(calc) ($Kwh\ m^{-2}$)	difference ($Kwh\ m^{-2}$)	%difference
June 11	7.51	7.98	+0.47	+6%
June 25	8.09	8.34	+0.25	+3%
July 9	7.78	7.71	-0.07	-1%
July 23	7.26	8.13	+0.87	+11%

(b) Daily totals of $L\downarrow$ measured and calculated by Swinbank's (1963) equation.

date	$L\downarrow$(meas) ($Kwh\ m^{-2}$)	$L\downarrow$(calc) ($Kwh\ m^{-2}$)	difference ($Kwh\ m^{-2}$)	%difference
June 25	3.41	3.84	0.43	12%
July 9	3.59	4.30	0.71	18%
July 23	3.61	4.10	0.49	13%
Aug. 15	3.79	4.07	0.28	7%
Sept.4	3.34	3.66	0.32	9%

(c) Mean hourly differences between measured and calculated $L\downarrow$.

Solar time:	0730	0830	0930	1030	1130	1230	1330	1430	1530	1630	1730
Difference: (Wm^{-2})	+6	-11	-39	-53	-69	-76	-70	-57	-50	-23	-8

FIGURE 4: MEASURED L↓ DEVIATION FROM SWINBANK'S FORMULA ON CLOUDLESS DAYS

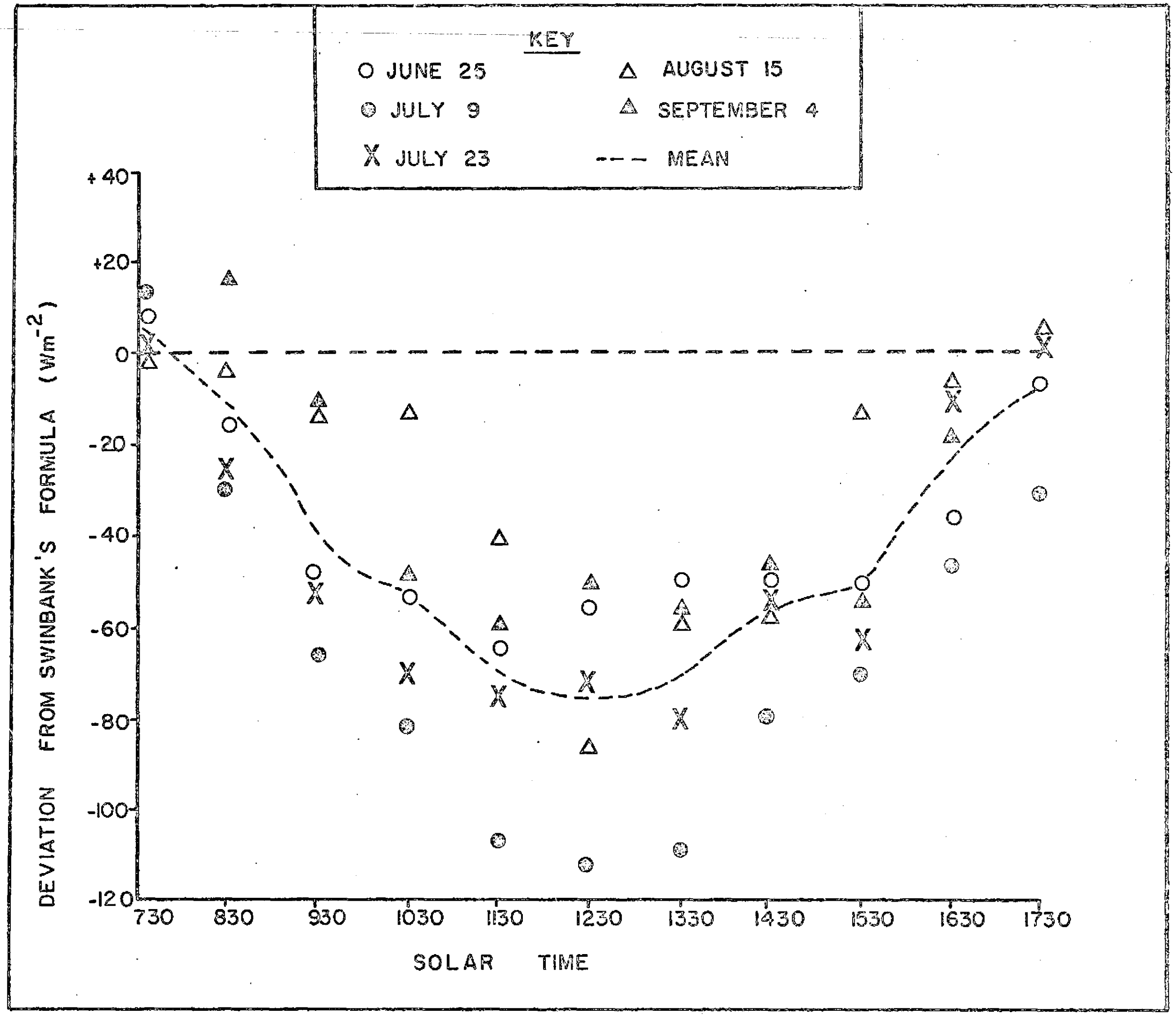

2. Diffuse radiation

A knowledge of the diffuse portion of the incident global radiation, $\delta = D/K\downarrow$, is a useful measure of sky conditions since the presence of clouds or haze increases δ. Measurements of diffuse radiation are underestimates since the shading ring obscures a significant portion of the sky. Drummond (1956) presented a theoretical correction factor which assumed isotropic radiation. This correction was evaluated. On overcast days, corrected diffuse measurements should be equal to measurements of incoming global radiation, unless a further correction for non-isotropy is necessary. Results from seven days with overcast periods indicate that measured and theoretical correction factors varied at most by 2.3% *(Table 3)*, contrary to the greater differences found by Davies et al (1970). A fixed correction factor of 11% based on the theoretical correction was therefore applied to all data.

Ratios of daily totals of diffuse to global radiation $\overline{\delta}$ were calculated. Cloudless day values were consistently lower than those for cloudy days *(Table 4)*. The highest $\overline{\delta}$ occurred on August 14, a predominantly overcast day.

The dependence of half-hourly values of δ on solar zenith angle *(Z)* on a cloudless day (June 25) is shown in *Figure 5*. The decrease of δ with decreasing Z is non-linear, reaching a minimum value at $Z = 40°$. Monteith (1973) considers a minimum ratio of 0.10 as characteristic of clear, dry air, 0.15 as most common for a cloudless day and 0.25 as characteristic of cloudless, dirty air. In this classification, June 25 was a very clear, dry day until about 1130

TABLE 3

CORRECTION FACTORS FOR DIFFUSE RADIATION MEASUREMENTS

date	sky condition	theoretical correction factor	measured correction factor (overcast)
June 11	cloudless	1.109	
June 19	cloudy	1.109	1.104
June 25	cloudless	1.109	
June 26	cloudy	1.109	1.124
July 3	cloudy	1.109	1.104
July 9	cloudless	1.109	
July 19	cloudless	1.111	
July 23	cloudless	1.111	
July 30	cloudy	1.112	1.133
Aug. 7	cloudy	1.112	
Aug. 12	cloudless	1.111	
Aug. 13	cloudy	1.111	1.106
Aug. 14	cloudy	1.111	1.139
Aug. 15	cloudless	1.111	
Aug. 27	cloudy	1.108	1.111
Sept.4	cloudless	1.104	
Sept.11	cloudless	1.100	

TABLE 4

MEAN DAILY RATIOS OF DIFFUSE TO GLOBAL RADIATION

date	sky condition	$\overline{\delta}$ (cloudless)	$\overline{\delta}$ (cloudy)
June 11	cloudless	0.284	
June 19	cloudy (sun at noon)		0.751
June 25	cloudless	0.150	
June 26	cloudy		0.764
July 9	cloudless	0.157	
July 23	cloudless (hazy)	0.344	
Aug. 7	cloudy		0.820
Aug. 12	cloudless	0.266	
Aug. 14	cloudy		0.921
Aug. 15	cloudless	0.412	
Aug. 27	cloudy		0.844
Sept. 4	cloudless	0.463	

FIGURE 5 : DEPENDENCE OF THE RATIO OF DIFFUSE TO GLOBAL RADIATION ON ZENITH ANGLE (JUNE 25)

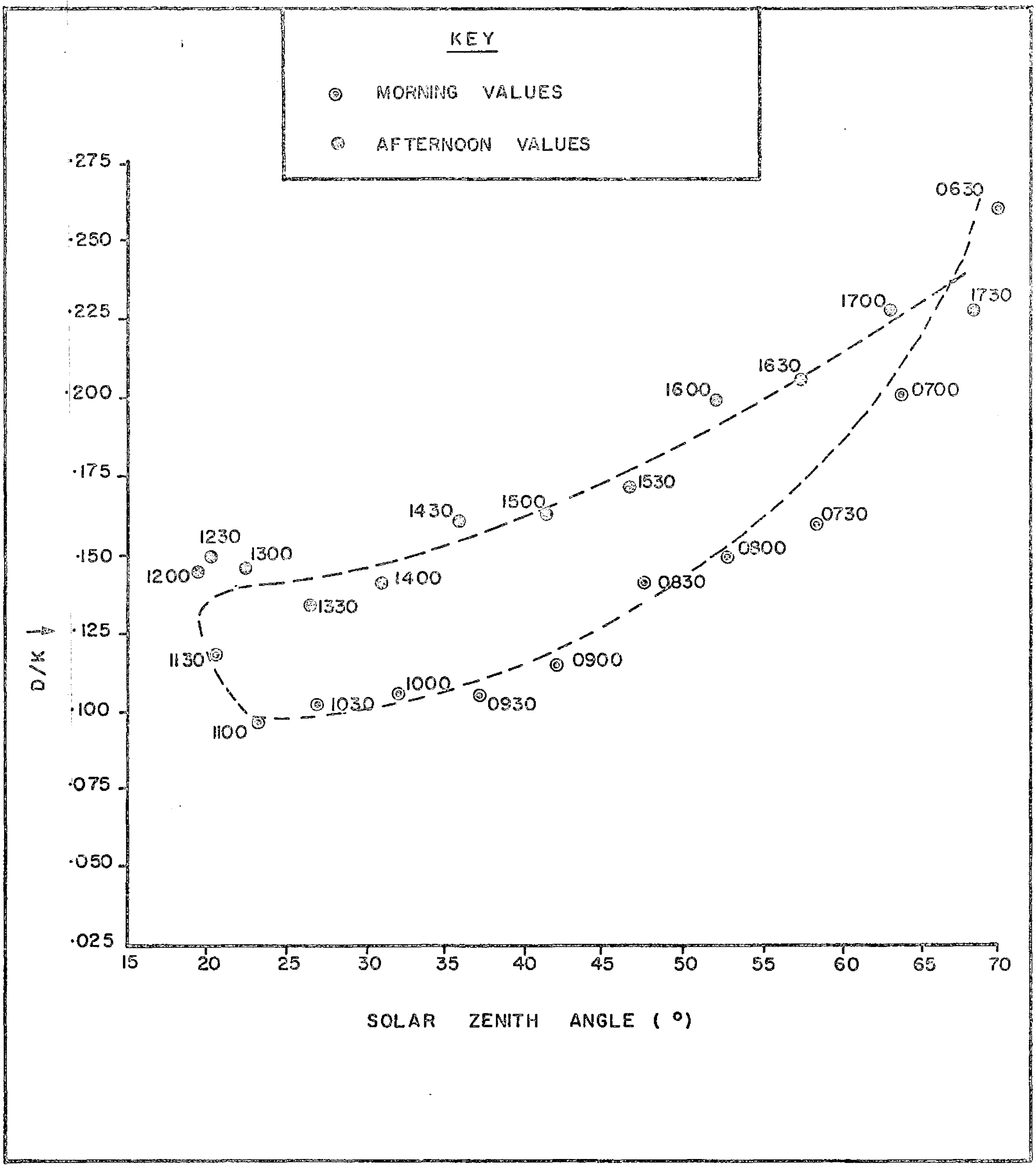

when a slight haze developed raising the value of δ to 0.15 by noon. Analysis of wind direction data *(Table 5)* indicates a change from predominately northerly winds from land to south-easterlies from Lake Erie at this time. Mukammal (1965) concluded that lake breezes and mesoscale wind systems brought pollution from the industrial regions of the United States to the south, up to the northern shores of Lake Erie causing weather fleck on tobacco plants near Delhi, 20 km west of Simcoe. The increase in δ observed here could also be caused by industrial pollution brought north via lake breezes, which often develop by midday.

3. <u>Reflection coefficient of the orchard</u>

Many researchers have found that the reflection coefficient of agricultural crops and other surfaces varies through the day, being least at solar noon and increasing with increasing solar zenith angle (Monteith and Szeicz, 1961; Davies and Buttimor, 1969; Impens and Lemeur, 1969a; Kyle, 1971; Proctor et al, 1972; Nkemdirim, 1973; and others). Fritschen (1967) argues that this diurnal variation can partly be attributed to sensor error. At low sun angles, energy is reflected within the hemispherical windshields of both upfacing and downfacing radiometers in approximately equal amounts thus resulting in large ratios. Idso, Baker and Blad (1969) support this conclusion although they still consider that a good portion of α variation is a real effect of the surfaces themselves.

A strong dependence of α on Z was found in this study on cloudless days *(Figure 6)*. On cloudy days, the dependence is weaker, as shown by the smaller values of the correlation and regression

TABLE 5

WIND DIRECTION AND SPEED AT SIMCOE, JUNE 25

EST	LAT	wind speed (mph)	wind direction (deg)	(direction)
0400	0337	05	001	N
0500	0437	04	341	NNW
0600	0537	04	344	NNW
0700	0637	05	051	NE
0800	0737	06	041	NE
0900	0837	07	067	ENE
1000	0937	05	122	SE
1100	1037	00	000	N
1200	1137	05	261	W
1300	1237	12	132	SE
1400	1337	12	158	SSE
1500	1437	08	153	SSE
1600	1537	09	161	SSE
1700	1637	06	143	SE
1800	1737	05	157	SSE
1900	1837	06	149	SSE
2000	1937	03	122	SE
2100	2037	05	128	SE

(EST = eastern standard time; LAT = local solar time)

FIGURE 6 : DEPENDENCE OF THE REFLECTION COEFFICIENT ON ZENITH ANGLE

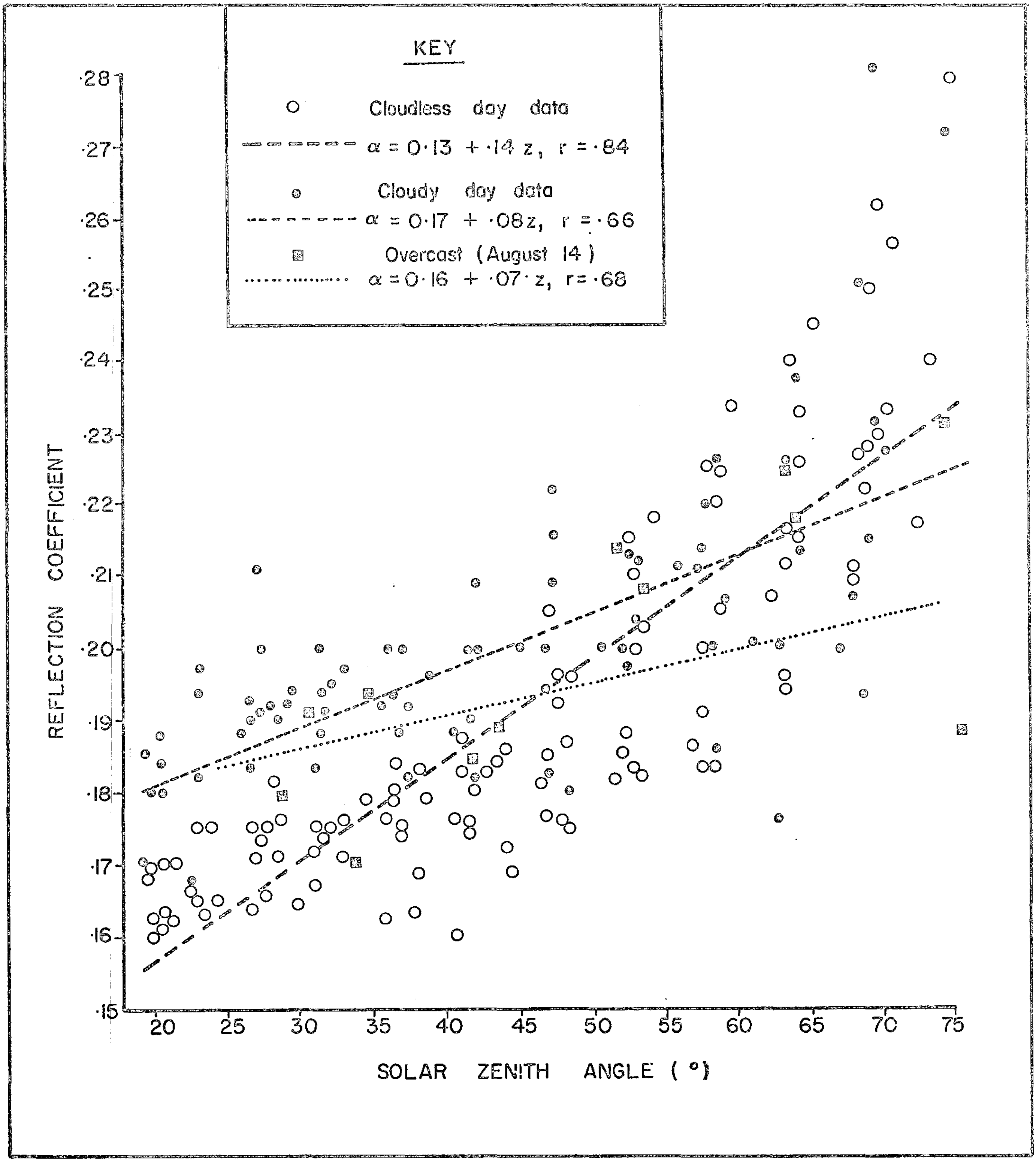

coefficients, due to the reduction in the direct beam radiation. August 14, an overcast day, had the smallest regression coefficient. Reflection of diffuse radiation has no angular dependence since the incoming energy is randomly distributed over the sky. Less dependence of α on Z for cloudy skies has also been observed by Impens and Lemeur (1969a) and Kyle (1971).

Pronounced increase in reflection at larger zenith angles is to be expected on cloudless days because optical laws indicate that more light will be reflected with increasing angle of incidence. Also, at large zenith angles, more of the incoming radiation is composed of NIR wavelengths, since during the longer path lengths through the atmosphere, shorter wavelength radiation is scattered. Plants reflect stronger in the infra-red (Monteith, 1959) causing higher reflection coefficients. Kalma and Badham (1972) concluded that spectral reflection is partially responsible for the increase in α for large Z although internal reflection within the sensors is also important. Increased penetration of light into crops at small zenith angles resulting in more trapping of radiation has also been cited as an important reason for the observed diurnal variation (Kalma and Stanhill, 1969).

Mean daily reflection coefficients $\bar{\alpha}$ were calculated as the ratio of the daily totals of $K\uparrow$ and $K\downarrow$. This method avoids the biased weighting by daily extremity values that occurs when the daily mean of hourly α values is evaluated. A time period of 0800 to 1600 was chosen for comparison with the results of Proctor et al (1972). In the present study, a difference exists between cloudless and cloudy days

(Figure 7) with higher α under cloudy skies. Mean reflection coefficient for the pooled data was 0.178 for cloudless days and 0.192 for cloudy days. The cloudless day mean is slightly higher than that reported by Proctor et al (0.162). Stanhill (1970) has related α to vegetation height showing that α decreases as height increases. This explains the higher reflection coefficient for the dwarf apple trees. These values compare with the following:

surface	α	reference
apple orchard	0.13-0.19	Landsberg, Powell and Butler (1973)
deciduous forests	0.159-0.181	Stanhill, Hofstede and Kalma (1966)
orange orchard	0.162	Kalma and Stanhill (1969)

4. Radiation balance relationships

The components of the radiation balance have been determined for sample cloudless and cloudy days *(Figures 8 and 9)*. Although absolute magnitudes varied, no seasonal trend in the relative patterns of the fluxes was evident for any terms when all cloudless and all cloudy days were compared. These results agree with those of Proctor et al (1972) and with other observations for a spruce forest (Tajchman, 1972) and a variety of crops (Monteith and Szeicz, 1961; Impens and Lemeur, 1969a; Kalma and Stanhill, 1969).

Monteith and Szeicz (1961) showed that net and net global radiation are linearly related:

$$Q^* = a + bK^*. \tag{6}$$

FIG. 7: SEASONAL VARIATION OF MEAN DAILY REFLECTION COEFFICIENTS.

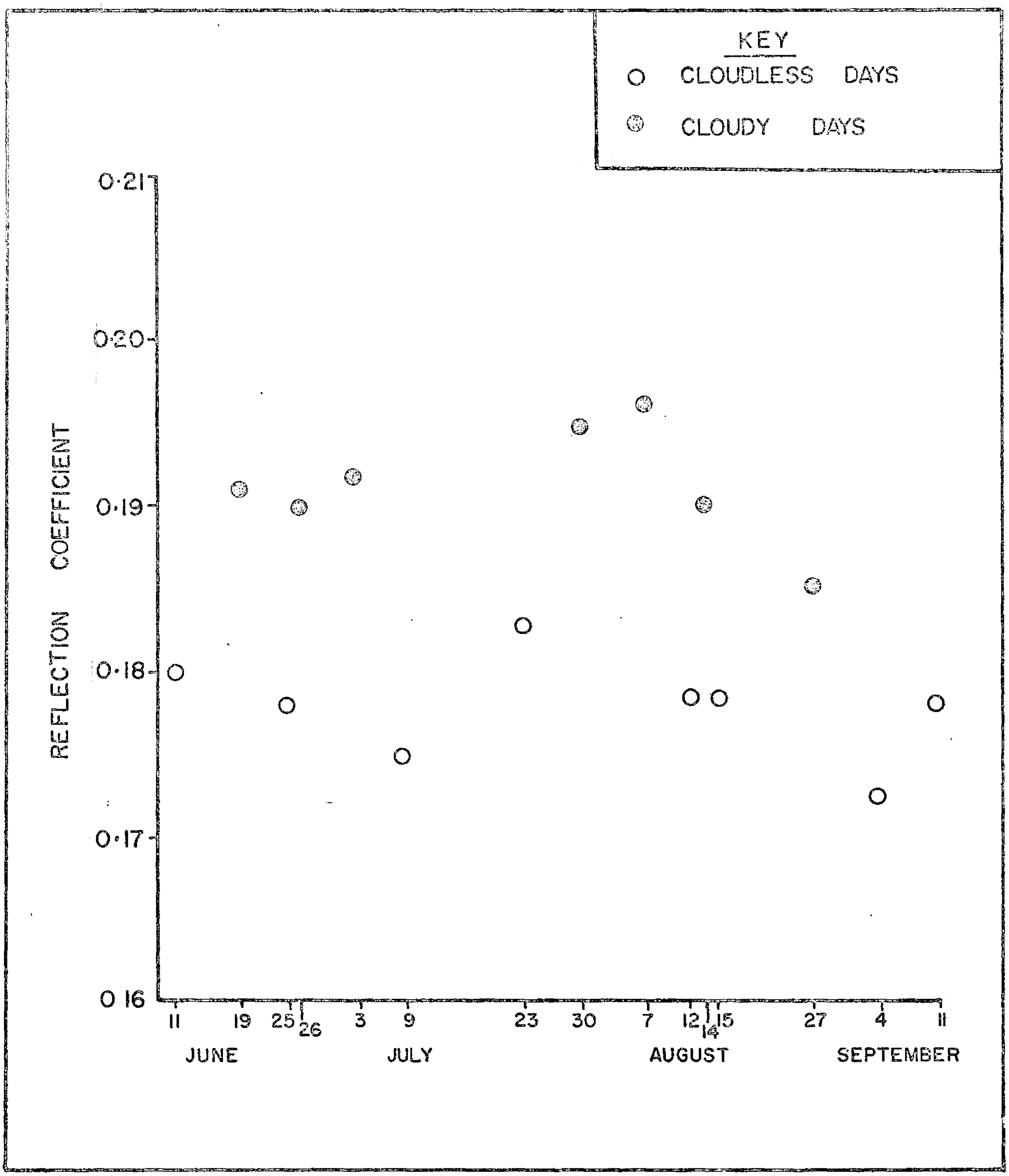

FIGURE 8: RADIATION BALANCE TERMS FOR A CLOUDLESS DAY (JUNE 25)

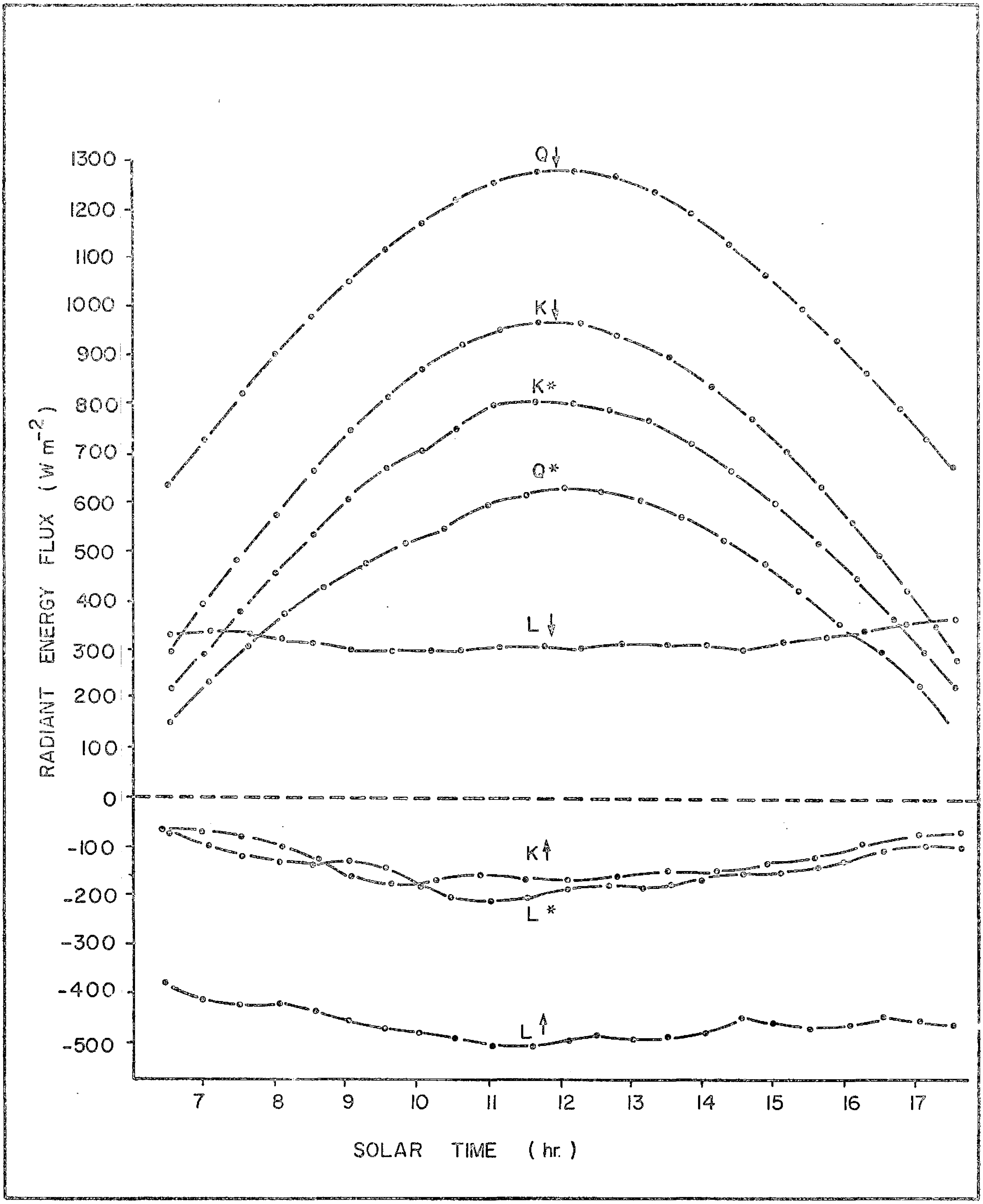

FIGURE 9: RADIATION BALANCE TERMS FOR A CLOUDY DAY (AUGUST 14)

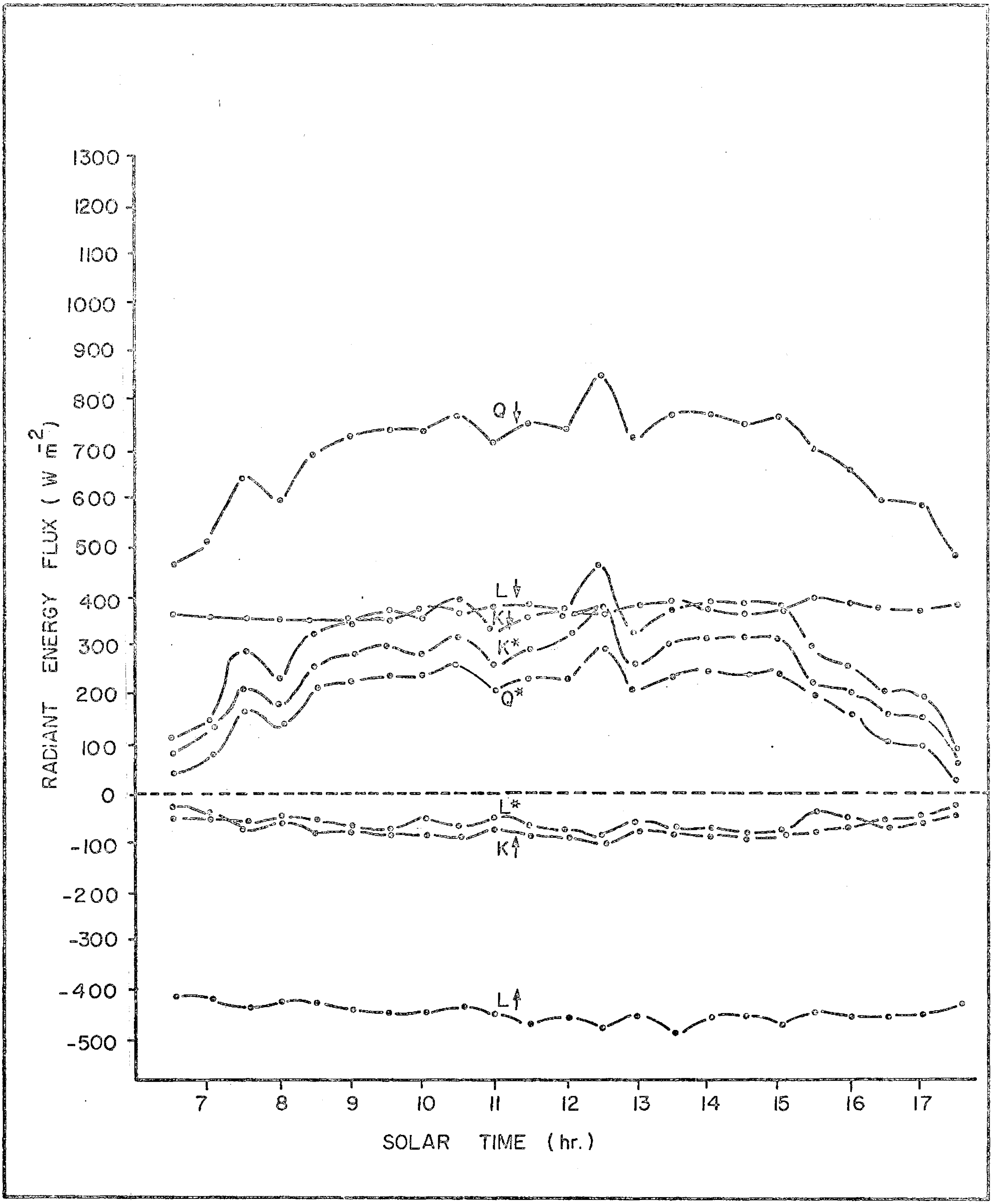

From the radiation balance (*equation 1)* and *equation 6*,

$$L^* = \frac{a}{b} - \frac{(1-b)}{b}\, Q^*. \tag{7}$$

Defining a heating coefficient $\beta = -dL^*/dQ^* = (1-b)/b$, $b = 1/(1+\beta)$ and *equation 6* becomes

$$Q^* = L^*(0) + \frac{K^*}{(1+\beta)}, \tag{8}$$

where $L^*(0)$ is the net terrestrial radiation at $K^* = 0$.

Regression and correlation analysis was used to obtain values of a and b for the apple orchard data *(Table 6)*. Correlation coefficients exceeded 0.992 for cloudless days and 0.985 for cloudy days. Heating coefficient values ranged between 0.112 and 0.348 with no apparent variation with cloud conditions *(Figure 10)*. These values compared favourably with those reported elsewhere for a variety of crops and surfaces (Monteith and Szeicz, 1961; Davies, 1967; Davies and Buttimor, 1969; Impens and Lemeur, 1969a; Nkemdirim, 1973). Negative β values reported by Stanhill et al (1966) and Idso et al (1969) were not found.

Landsberg et al (1973) obtained β values for an apple orchard ranging from 0.2 to 0.6 with an average value of 0.305 obtained from 4 monthly values. Results for a single tree (Proctor et al, 1972) ranged from 0.101 to 0.380 under cloudless skies. Pooling their data, they obtained

$$Q^* = -42 + 0.86\, K^*, \quad r = 0.98, \tag{9}$$

TABLE 6

REGRESSION AND CORRELATION ANALYSIS OF Q^* UPON K^* AND L^* UPON K^*

(a = intercept, b = regression coefficient, r = correlation coefficient)

date	Q^* upon K^*				L^* upon K^*			
	a	b	r	β	a	b	r	λ
cloudless:								
June 25	−17	.79	.997	.269	−17	−.21	.959	−.212
July 9	−6	.74	.996	.348	−6	−.26	.972	−.258
July 23	−27	.80	.997	.244	−27	−.20	.949	−.196
Aug. 12	−38	.87	.995	.149	−38	−.13	.908	−.130
Aug. 15	−33	.85	.996	.183	−33	−.16	.909	−.155
Sept. 4	−20	.85	.992	.175	−20	−.15	.891	−.149
cloudy:								
June 19	+10	.78	.985	.285	+10	−.22	.853	−.222
June 26	−4	.84	.994	.203	−4	−.17	.876	−.165
Aug. 7	−33	.89	.994	.125	−33	−.11	.737	−.111
Aug. 14	−29	.90	.993	.112	−29	−.10	.673	−.100
Aug. 27	+7	.78	.990	.284	+7	−.22	.891	−.221
All days	−4	.786	.992	.272	−4	−.214	.901	−.214

FIGURE 10: SEASONAL VARIATION OF THE HEATING AND LONGWAVE EXCHANGE COEFFICIENTS

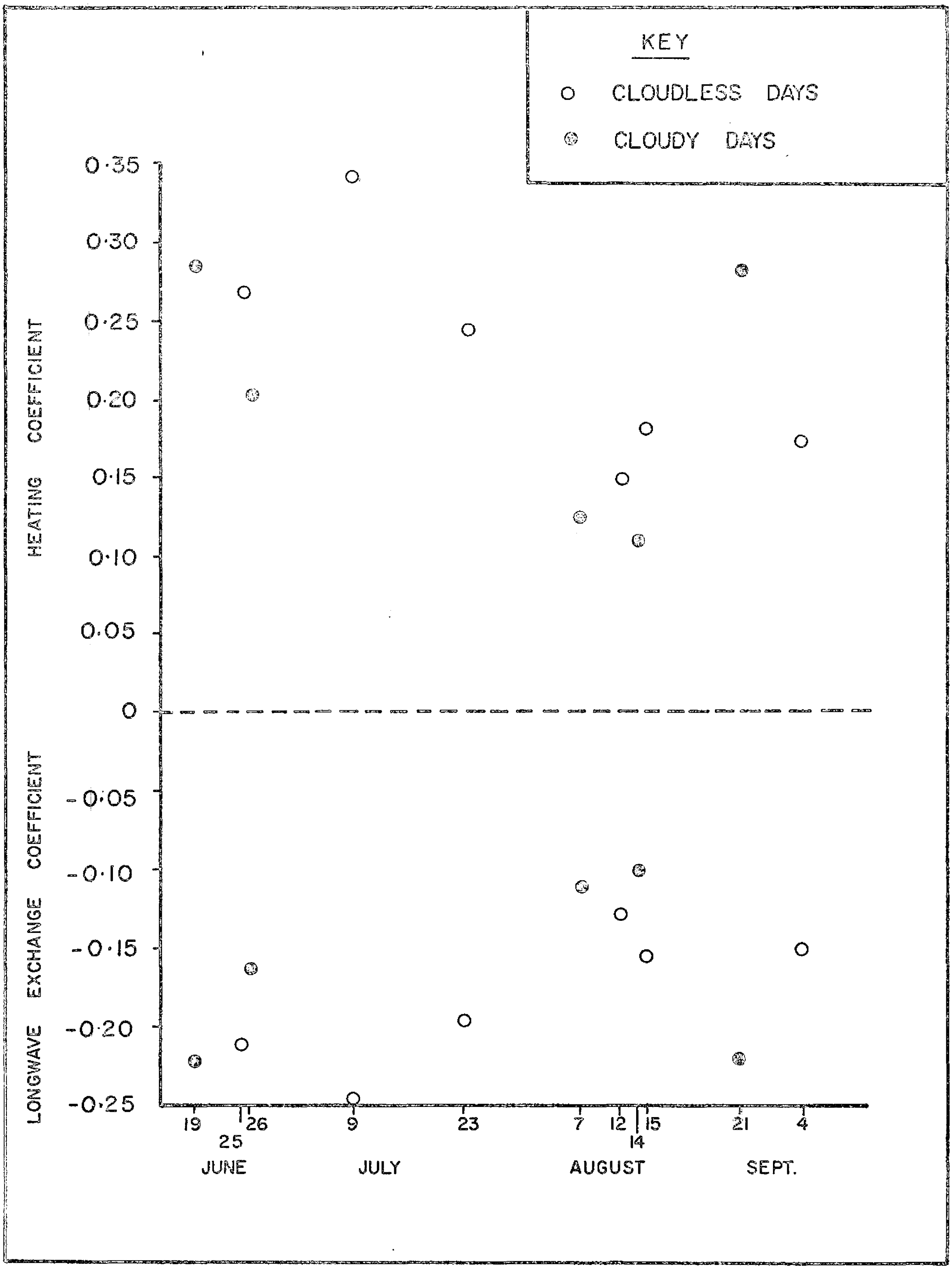

with $\beta = 0.165$. When the present data are pooled,

$$Q^* = -4 + 0.786\,K^*, \quad r = 0.99, \tag{10}$$

with $\beta = 0.272$. This value differs by 0.03 from that of Landsberg et al and by 0.11 from the Proctor et al result. The significance of these differences in β ($d\beta$) to Q^* estimation was analysed. Differentiating *equation 8*,

$$\frac{dQ^*}{Q^*} = \frac{-d\beta}{1+\beta}\left[1 + \frac{L^*(0)}{K^*}(1+\beta)\right]^{-1}. \tag{11}$$

For $d\beta = 0.03$, $0.05 < \beta < 0.4$ and $-0.15 < L^*(0)/K^* < 0.05$, which includes the present values, $0.02 < dQ^*/Q^* < 0.03$. For $d\beta = 0.11$ and the same ranges of β and $L^*(0)/K^*$, $0.07 < dQ^*/Q^* < 0.12$. Thus, the differences between the mean β value in the present study and those reported in the other two studies result in 2-3% and 7-12% differences in Q^* estimation respectively. Since Q^* cannot be measured to an accuracy better than 10%, these β differences are not significant.

Gay (1971) has noted that the statistical relationship between Q^* and K^* used to define a heating coefficient is difficult to justify. From *equations 1* and *6*,

$$K^* + L^* = a + bK^*. \tag{12}$$

Hence, in the regression, K^* appears as a component in the dependent variable. It follows that high correlations must exist between Q^* and K^* which depend on the perfect correlation between K^* and itself. Removing K^* from the left hand side of *equation 12*,

$$L^* = a + (b-1)\ K^*. \tag{13}$$

He defined a longwave exchange coefficient λ as the regression coefficient in the linear relationship between L^* and K^*. Hence,

$$L^* = L^*(0) + \lambda\ K^*. \tag{14}$$

For the apple orchard, correlation coefficients between L^* and K^* exceeded 0.9 on all cloudless days except one, but were less on cloudy days *(Table 6)*. Values of λ ranged from -0.100 to -0.258 with no detectable difference between cloudless and cloudy days *(Figure 10)*. Proctor et al (1972) report a similar range of λ between -0.090 and -0.276 with a mean of -0.142. Pooling the present data,

$$L^* = -4 - 0.214\ K^*, \quad r = 0.90. \tag{15}$$

The difference between the two λ values $(d\lambda)$ is 0.07. The significance of λ differences to L^* estimation was tested by differentiating *equation 14:*

$$\frac{dL^*}{L^*} = d\lambda \left[\lambda + \frac{L^*(0)}{K^*} \right]^{-1}. \tag{16}$$

For $d\lambda = 0.07$, $-0.30 < \lambda < -0.09$ and $-0.15 < L^*(0)/K^* < 0.05$, $-0.16 < dL^*/L^* < -1.75$. This represents a difference of 16 to 175% in L^* estimation. Hence, small variations in λ are significant since they produce large differences in L^* estimation. The importance of this error may, however, be small in Q^* estimations since K^* is the dominant term in *equation 1*.

CHAPTER IV

TRANSMITTED GLOBAL RADIATION

1. Introduction

Within a plant community, the transmission of radiation is variable both in time and space. Temporal variations are caused by changes in the sun's position in the sky and by changes in plant growth. Spatial sources of variation include the presence of gaps in the vegetation which produce sunflecks, the swaying of foliage in the wind, and the transmission and scattering properties of the plants. Since there is variability in the radiation received beneath a canopy, radiation measurements should be averaged over both space and time. This requires either the use of many sensors (Anderson, 1966; Impens and Lemeur, 1969b) or an integrating sensor such as a linear pyranometer (Kyle, 1971) or a moving sensor. The latter have the advantages of lower cost, since only one sensor is needed, and extensive spatial coverage. In the present study, both stationary sensors and a traversing sensor were used.

2. Comparison between measurements from stationary and traversing sensors

Ten stationary pyranometers measured transmitted radiation during the ten minute traverse period. During this time, approximately 25 signals were received from each stationary sensor. The mean and standard deviation for each sensor and a pooled mean and standard deviation for the ten pyranometers were obtained. Examples are shown for a cloudless and cloudy ten minute period in *Table 7*. Standard deviations are higher for the cloudless period being 1.4 to 11.8% for individual sensors and 52.3% between all sensors. Under cloud, the greatest individual standard deviation is 3.8% while between all ten sensors, standard deviation is 20.9%. Mean transmission results for the cloudless traverse from the moving and stationary sensors differed by 25.7% (496 Wm^{-2} compared to 642 Wm^{-2}) while for the cloudy period, only 1.6% (251 Wm^{-2} compared to 255 Wm^{-2}). In both cases, the moving sensor mean is well within the standard deviation of the stationary sensor mean.

Hourly transmission coefficients (τ) for both the stationary and moving sensor results were calculated ($\tau = K_T/K\downarrow$) for three cloudless and three cloudy days *(Figures 11 and 12)*. The stationary sensors were relocated for the third cloudless and cloudy day to compare the behaviour of two different grids with the results from the traversing sensor. No diurnal variation in the behaviour of τ on cloudless days for the stationary sensor results was discernible; whereas, the moving sensor showed a peak around noon. On cloudy days, the variations from both measuring systems were similar but τ calculated from the stationary sensors is consistently greater. Relocation of the stationary grid did not affect this conclusion.

Mean daily transmission coefficients were calculated from $\bar{\tau} = \Sigma\, K_T/\Sigma K\downarrow$ with the stationary sensor results calculated as a mean of the ten individual daily sensor means. The stationary sensor values

TABLE 7

SAMPLE RESULTS OF K_T FROM STATIONARY SENSORS

July 9, 1030 (cloudless)

sensor #	mean (Wm^{-2})	standard dev. (Wm^{-2})	standard dev. (%)
1	900	85	9.5
2	926	24	2.6
3	416	49	11.8
4	820	58	7.1
5	945	18	1.9
6	925	13	1.4
7	822	56	6.8
8	154	7	4.7
9	396	33	8.3
10	111	3	3.0
all ten	642	336	52.3

June 26, 1030 (cloudy)

sensor #	mean (Wm^{-2})	standard dev. (Wm^{-2})	standard dev. (%)
1	296	8	2.8
2	305	7	2.4
3	325	9	2.8
4	251	4	1.6
5	266	10	3.8
6	313	8	2.5
7	197	4	2.2
8	202	3	1.3
9	197	5	2.4
10	196	5	2.6
all ten	255	53	20.9

FIGURE II: CLOUDLESS DAY TRANSMISSION COEFFICIENTS FROM MOVING AND STATIONARY SENSORS

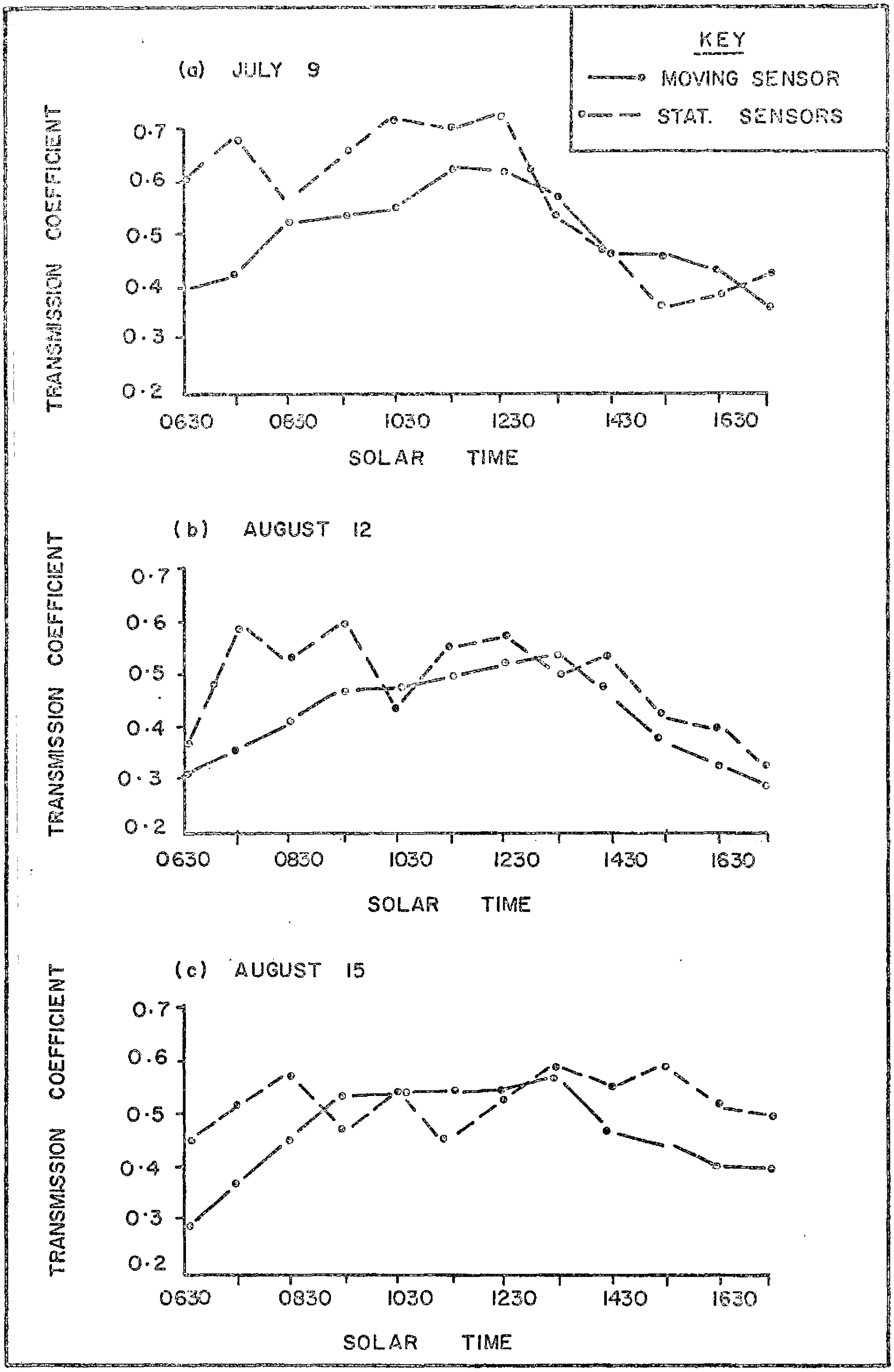

FIGURE 12: CLOUDY DAY TRANSMISSION COEFFICIENTS FROM MOVING AND STATIONARY SENSORS

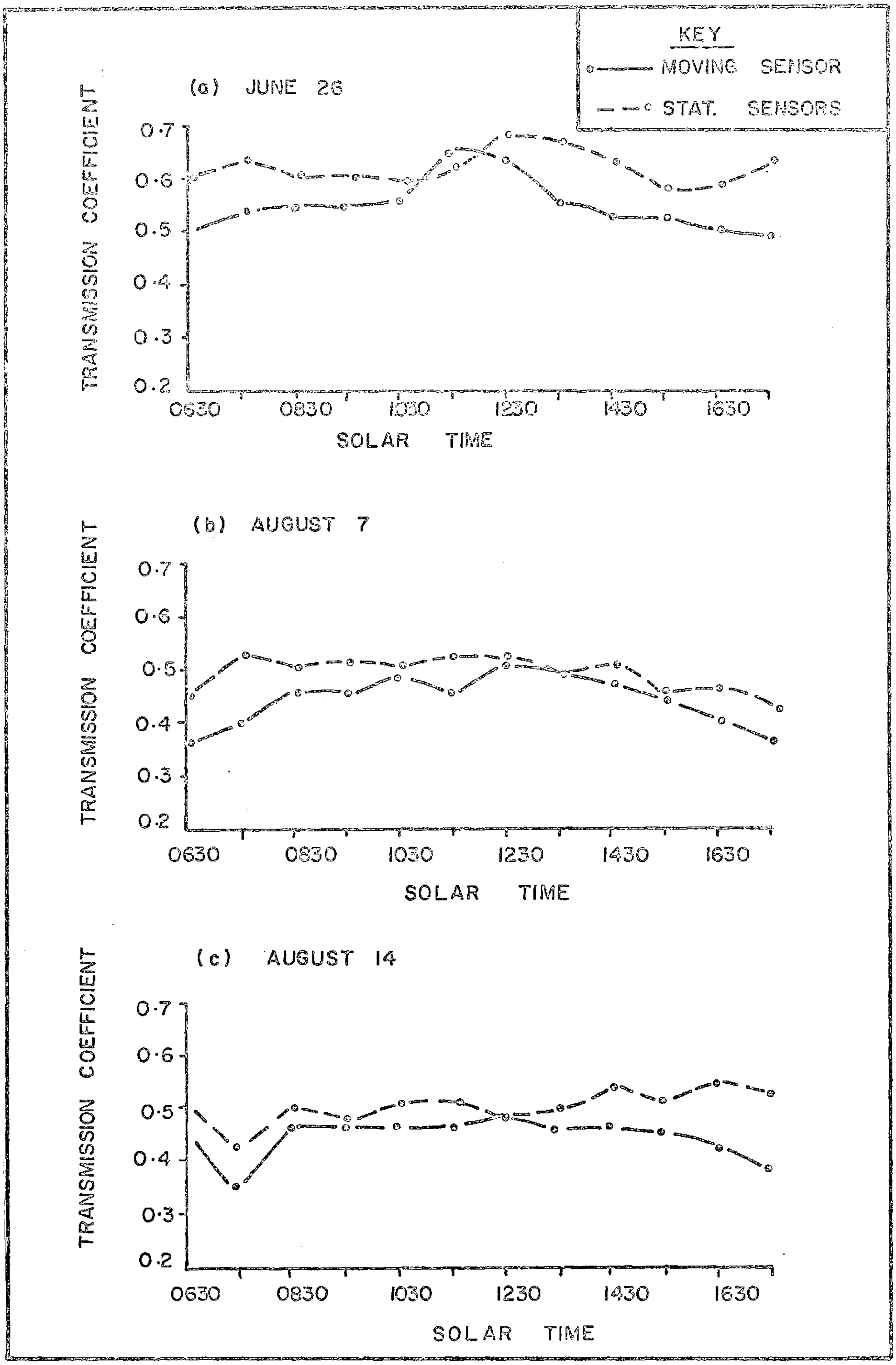

TABLE 8

MEAN DAILY TRANSMISSION COEFFICIENTS CALCULATED FROM MOVING AND STATIONARY SENSOR MEASUREMENTS

date	$\overline{\tau}$ (stationary)	$\overline{\tau}$ (moving)	$\Delta \overline{\tau}$	% difference
cloudless:				
July 9	0.59 (σ = 31.7%)	0.53	0.06	10.7%
Aug. 12	0.51 (σ = 31.4%)	0.45	0.06	12.5%
Aug. 15	0.53 (σ = 30.4%)	0.51	0.02	3.8%
cloudy:				
June 26	0.64 (σ = 23.1%)	0.58	0.06	9.8%
Aug. 7	0.49 (σ = 23.0%)	0.46	0.03	6.4%
Aug. 14	0.51 (σ = 11.9%)	0.49	0.02	4.0%

were consistently higher *(Table 8)*. Agreement between the two methods of measurement improved for the second location of the stationary sensors. Standard deviations for the means of the stationary sensors were higher on cloudless days. Changing the location of the grid lowered the standard deviation only slightly on August 15. The low standard deviation on August 14 compared with the other two cloudy days can be attributed to the fact that this day was predominately overcast. This indicates that relocation of the stationary sensors did not reduce the variation among the individual sensors themselves, but the overall mean was in closer agreement with the moving sensor. Reifsynder, Furnival and Horowitz (1971) and Mukammal (1971) found that a stationary grid of a 'sufficient' number of sensors yielded satisfactory results on a daily basis. Here, using the traverse results for comparison, ten sensors were sufficient for a daily estimate of global radiation transmission only for the second grid.

3. The partitioning of incident global radiation

The global radiation incident upon the orchard can be partitioned into reflected, transmitted, and absorbed components. As previously discussed, reflected and transmitted global radiation are measured directly. Since absorption of transmitted radiation reflected up to the foliage from the soil surface is small due to the small magnitude of such reflection, the absorbed component is computed from

$$K_A = K\downarrow - K\uparrow - K_T. \tag{17}$$

Hence, the absorption coefficient is

$$\phi = 1 - \tau - \alpha. \tag{18}$$

Representative examples for a cloudless and cloudy day are shown in *Figure 13.* The transmitted and reflected components were respectively the largest and the smallest portions of incident global radiation.

Transmission coefficients showed diurnal trends with peak values at noon. This has been observed by Kalma and Stanhill (1969) in an orange plantation, Mukammal (1971) in a pine forest, and others in a variety of crops. Strong correlation between τ and Z is shown in *Figures 14 and 15.* Correlation coefficients exceed 0.90 on cloudless days and range between 0.78 and 0.94 on cloudy days. Variation of τ was greatest on cloudless days as indicated by the regression coefficients which ranged from -0.40 to -0.55. On cloudy days, regression coefficients were smaller ranging from -0.24 to -0.45, with August 14, a predominately overcast day, only -0.20. Variations in the dependence of τ on Z may be explained by differences in sky conditions i.e. degree of cloudiness or presence of haze as indicated by $\overline{\delta}$ values, and by the stage of development of the foliage.

Since both α and τ depend linearly on Z, it follows that the absorption coefficient should also depend linearly on Z. Correlation and regression coefficients, however, were lower *(Table 9)* indicating that such dependence is not as strong.

Mean daily coefficients have been calculated for all three components *(Table 10).* A seasonal trend for $\overline{\tau}$ and $\overline{\phi}$ was observed

FIGURE 13: DIURNAL PARTITIONING OF K↓

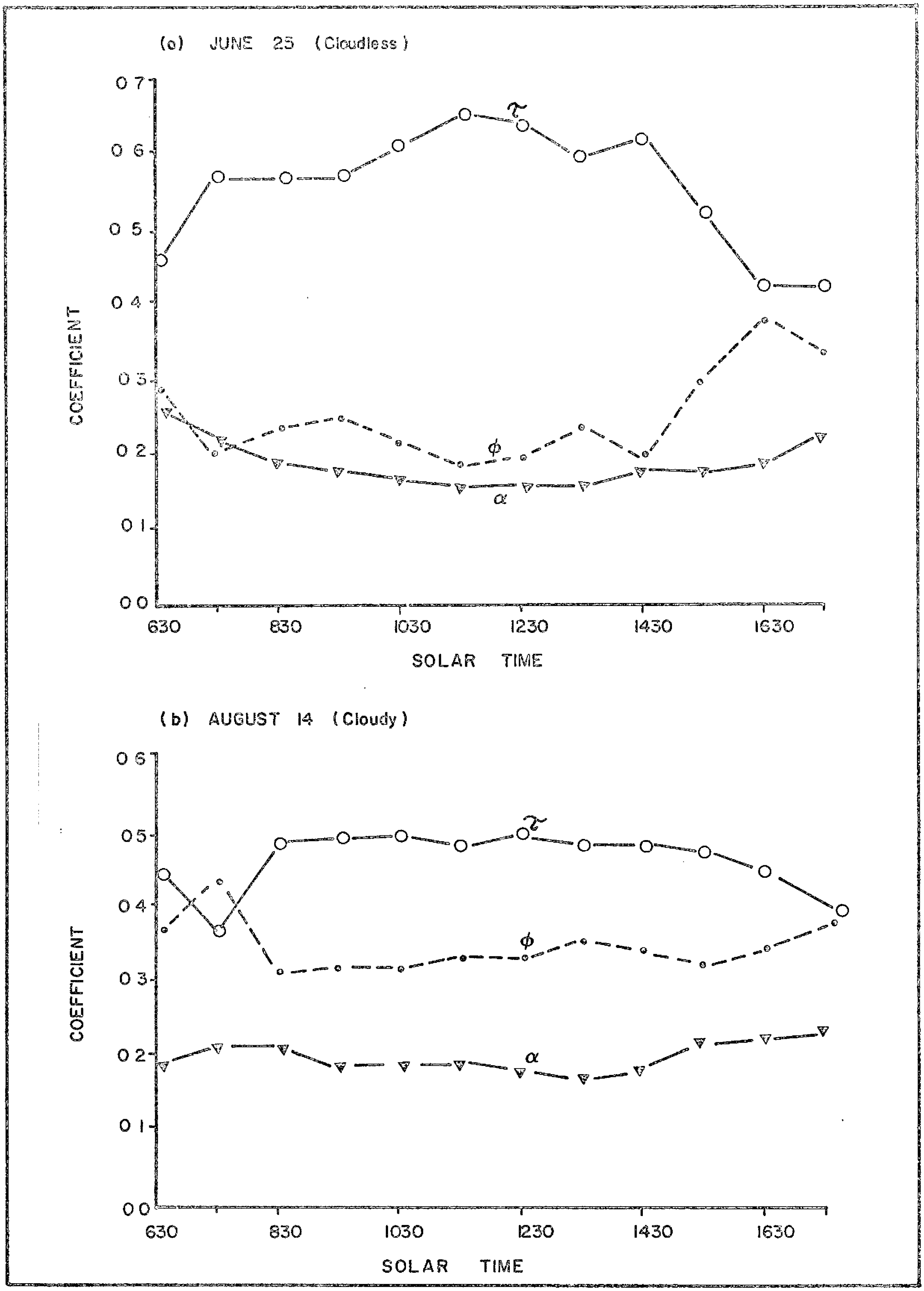

FIGURE 14: DEPENDENCE OF THE TRANSMISSION COEFFICIENT ON SOLAR ZENITH ANGLE ON CLOUDLESS DAYS.

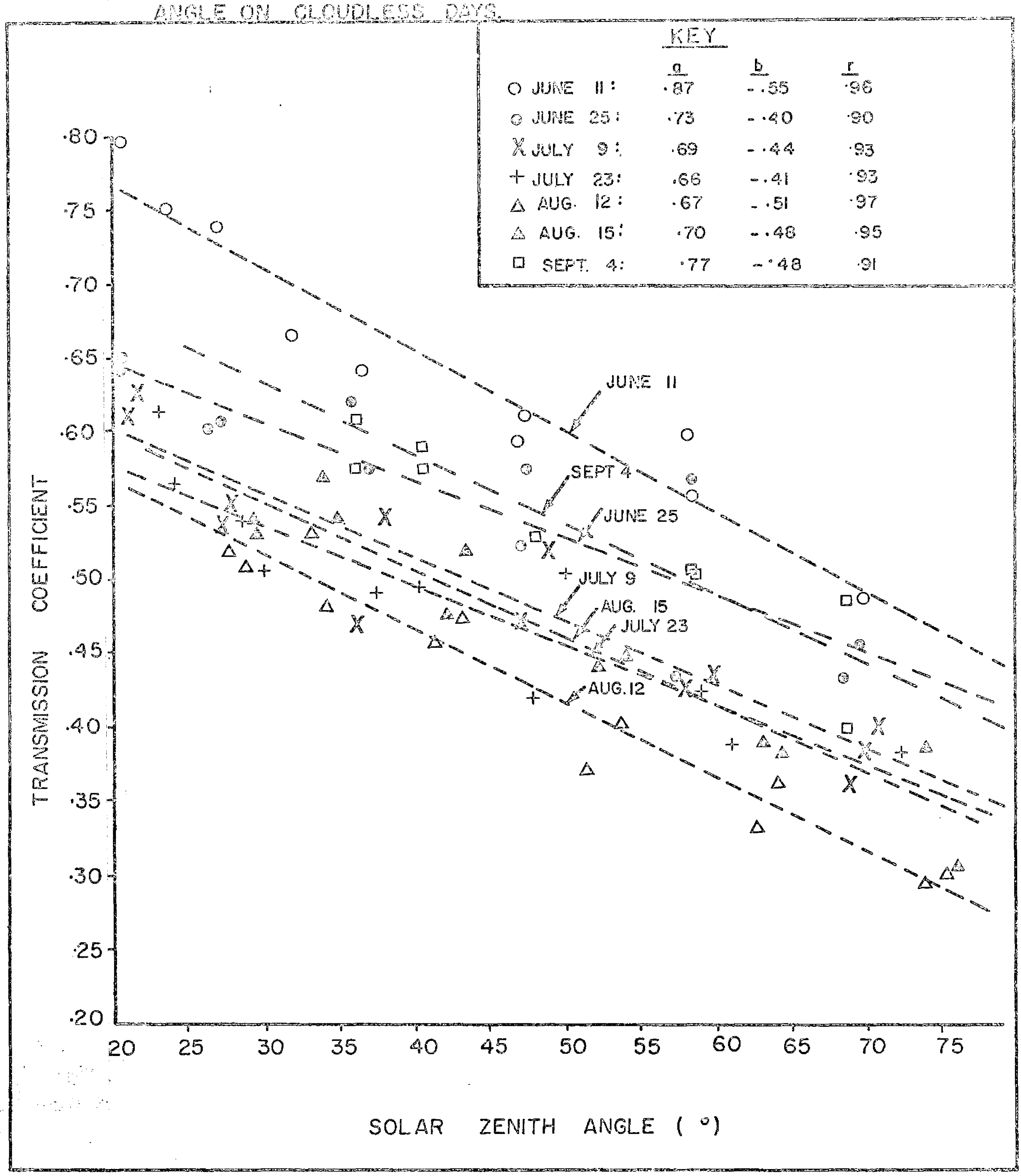

FIGURE 15: DEPENDENCE OF THE TRANSMISSION COEFFICIENT ON SOLAR ZENITH ANGLE ON CLOUDY DAYS

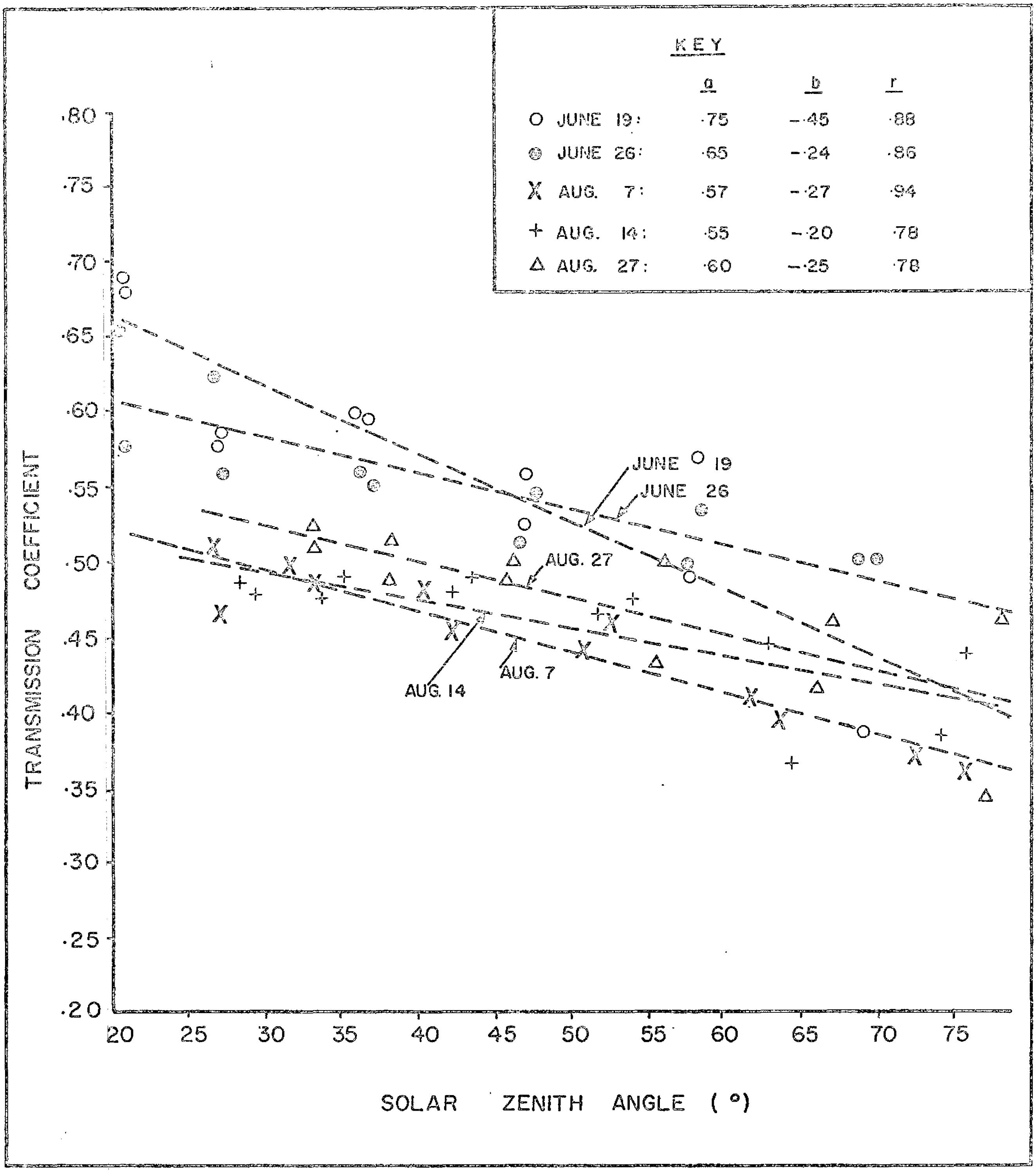

TABLE 9

REGRESSION AND CORRELATION ANALYSIS TO SHOW THE DEPENDENCE OF THE ABSORPTION COEFFICIENT ON ZENITH ANGLE

(a = intercept, b = regression coefficient, r = correlation coefficient.)

	a	*b*	*r*
cloudless days:			
June 11	-0.01	0.40	0.90
June 25	0.15	0.23	0.69
July 9	0.18	0.29	0.84
July 23	0.20	0.28	0.81
Aug. 12	0.20	0.36	0.89
Aug. 15	0.18	0.30	0.94
Sept.4	0.12	0.34	0.78
cloudy days:			
June 19	0.05	0.42	0.91
June 26	0.19	0.10	0.43
Aug. 7	0.26	0.18	0.70
Aug. 14	0.30	0.09	0.37
Aug. 27	0.25	0.16	0.72

TABLE 10

THE PARTITIONING OF $K\downarrow$ DAILY TOTALS

date	$K\downarrow$ ($Kwh\ m^{-2}$)	$K\uparrow$ ($Kwh\ m^{-2}$)	K_T ($Kwh\ m^{-2}$)	K_A ($Kwh\ m^{-2}$)	$\overline{\alpha}$	$\overline{\tau}$	$\overline{\phi}$
cloudless:							
June 11	7.51	1.35	5.04	1.12	.18	.67	.15
June 25	8.09	1.46	4.69	1.94	.18	.58	.24
July 9	7.78	1.40	4.02	2.26	.18	.53	.29
July 23	7.26	1.31	3.62	2.33	.18	.50	.32
Aug. 12	7.13	1.28	3.21	2.64	.18	.45	.37
Aug. 15	5.67	1.01	2.89	1.77	.18	.51	.31
Sept. 4	4.64	0.78	2.54	1.32	.17	.55	.28
mean					.18	.54	.28
cloudy:							
June 19	5.22	1.00	3.12	1.10	.19	.60	.21
June 26	4.60	0.88	2.66	1.04	.19	.58	.23
Aug. 7	4.79	0.91	2.19	1.69	.19	.46	.35
Aug. 14	3.51	0.66	1.71	1.14	.19	.49	.32
Aug. 27	2.76	0.53	1.33	0.90	.19	.48	.33
mean					.19	.52	.29
mean all days					.185	.53	.285

(Figure 16) with minimum values of $\bar{\tau}$ and maximum $\bar{\phi}$ occurring in mid-August. This corresponds to the maximum extent of leaf development. In late August and early September, dry weather caused some leaves to fall, thus raising $\bar{\tau}$ values. Values of $\bar{\tau}$ were consistently above 0.45 with a mean of 0.53 for the pooled data. Kalma and Stanhill (1969) found a similar seasonal trend for an orange plantation with $\bar{\tau}$ ranging from a minimum of 0.13 in August to a maximum of 0.36 in October with a mean of 0.21. For deciduous forests, seasonal values of 0.17 (Schomaker, 1968) and 0.10-0.12 (Vézina and Grandtner, 1965) have been reported. The higher values in the present study indicate a less dense foliage and, hence, less absorption.

No apparent difference existed between cloudless and cloudy day values of $\bar{\tau}$ and $\bar{\phi}$ *(Table 10)*. Differences between cloudless and cloudy day values of $\bar{\alpha}$ *(Figure 7)*, are insignificant in the calculation of absorption coefficients.

As an average for the entire study period, 18.5% of the incident global radiation was reflected from the canopy, 53% was transmitted, and 28.5% was absorbed by the trees.

FIGURE 16: SEASONAL VARIATION OF THE REFLECTION, TRANSMISSION AND ABSORPTION COEFFICIENTS

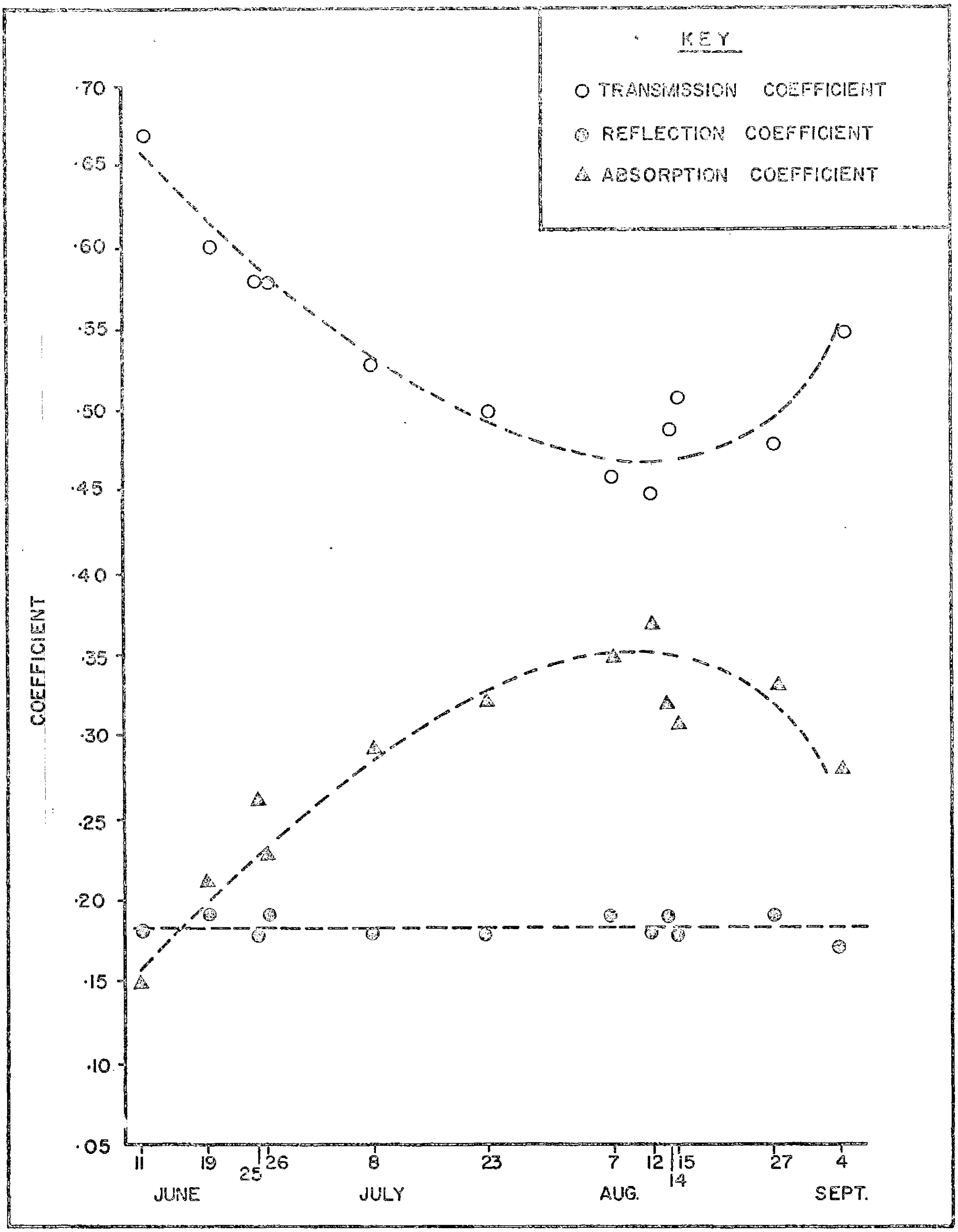

CHAPTER V

PHOTOSYNTHETICALLY ACTIVE RADIATION

1. Incident and reflected PAR

Values of the ratio $K_p\downarrow/K\downarrow$ range between 0.39 and 0.47 for cloudless skies and are usually higher on cloudy days (Yocum, Allen and Lemon, 1964; Monteith, 1965; Szeicz, 1966; Paltridge 1970b; Efimova, 1971). Recently, Szeicz (1970) found a ratio of 0.50 from theory and from experimental data. Further, he found little evidence for seasonal or diurnal variation. The ratio increased to between 0.51 and 0.53 at high δ values (i.e. 8/10 cloud cover or more).

To establish a relationship whereby $K_p\downarrow$ could be calculated from $K\downarrow$, PAR was measured on eight cloudless and one overcast day. Linear regression analysis was used to relate $K_p\downarrow$ and $K\downarrow$ *(Figure 17)*. For the cloudless days

$$K_p\downarrow = 0.49\ K\downarrow - 12, \quad r = 0.999, \tag{19}$$

and for the overcast day

$$K_p\downarrow = 0.50\ K\downarrow - 4, \quad r = 0.995. \tag{20}$$

The values of the regression coefficients, 0.49 on cloudless days and 0.50 for overcast, represent the ratios $K_p\downarrow/K\downarrow$ since the intercepts are

FIGURE 17 : RELATIONSHIP OF INCIDENT PAR AND GLOBAL RADIATION

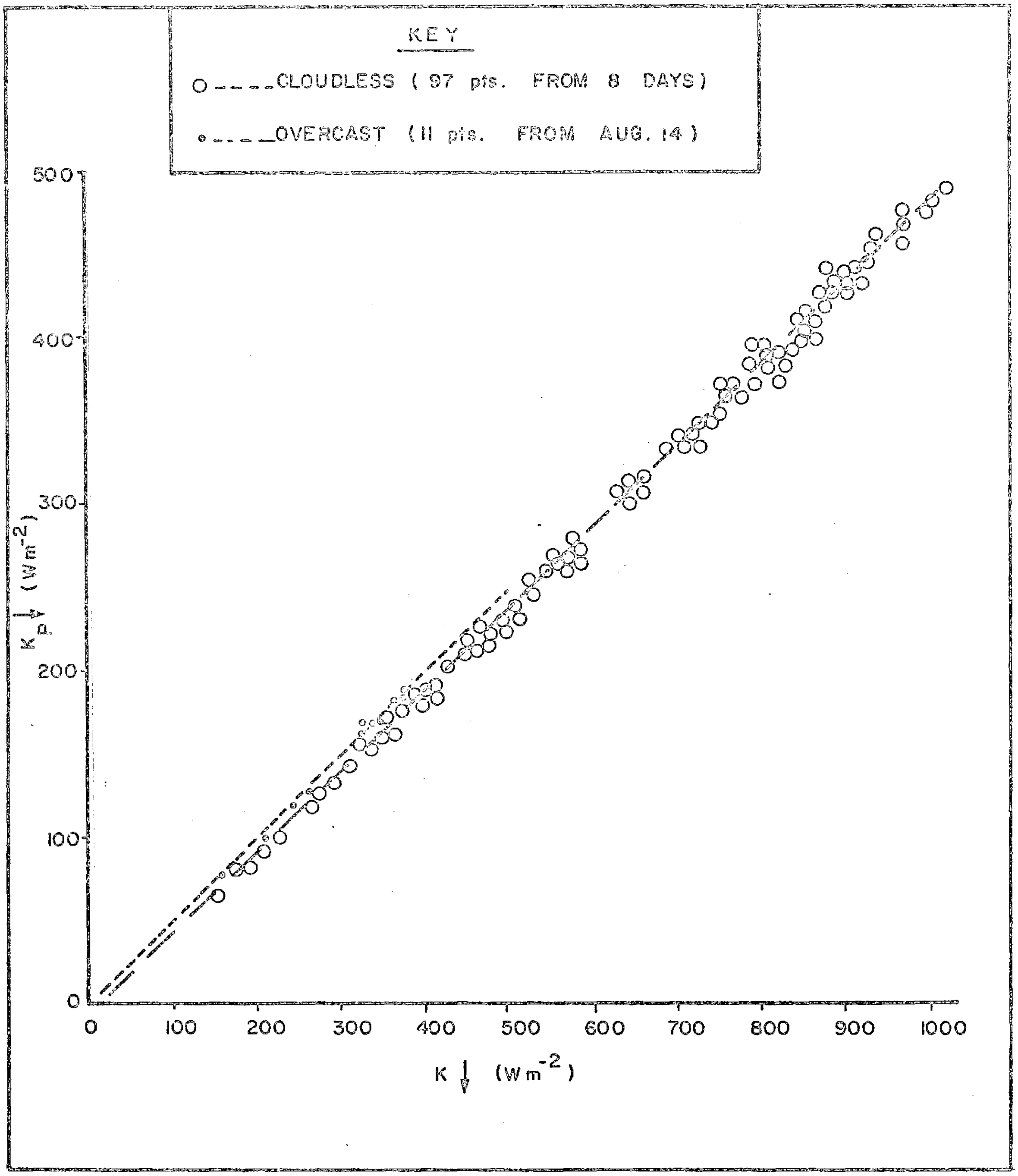

close to zero. These results agree very closely with those of Szeicz (1970). Since the relationship is sufficiently linear and the correlation coefficients are high, *equations 19 and 20* could be used to predict $K_p\downarrow$ from $K\downarrow$. However, measurements from only one overcast day were available and the results of *equations 19 and 20* are similar. Therefore, *equation 19* was used to calculate hourly values of $K_p\downarrow$ on all days for the analysis in section 2.

For an individual leaf, reflectance differs considerably between the PAR and NIR portions of the global radiation spectrum, being much lower for PAR (Monteith, 1959; Gates, 1965). When considering a complete plant canopy, the geometry of the canopy and the angle of incidence of the sun as well as the radiative properties of the individual leaves are important. Myers and Allen (1968) have shown differences for spectral reflectance from individual leaves and a canopy due to multiple reflection and trapping of radiation in the canopy. Nevertheless, for the entire canopy, the PAR reflection coefficient (α_p) is much lower and, hence, the NIR reflection coefficient much higher than the overall α for global radiation.

Some reported values of α_p are listed below:

surface	α_p	reference
corn	.07	Yocum et al, 1964
alfalfa	.06	Yocum et al, 1964
forests	.05 to .20	Monteith, 1959
forests	.03 to .05	Bray, Sanger and Archer, 1966
grass	.06 to .08	Bray et al, 1966

A dependence on solar zenith angle has been shown. As with α, α_p increases with zenith angle (Bray et al, 1966; Coulson and Reynolds, 1971).

Since measurements of reflected PAR ($K_p\uparrow$) were not made, α_p for the orchard was assumed to range from 0.06 to 0.09 during the day with a mean daily value of $\alpha_p = 0.07$, based upon the above values. Seasonal variation was neglected.

2. Transmission and partitioning of incident PAR

Analysis of the partitioning of $K_p\downarrow$ was similar to that for $K\downarrow$. Only transmitted PAR (K_{pT}) was measured directly. The reflected component was determined using the assumptions of the preceeding section. Absorbed PAR was evaluated as the residual from

$$K_{pA} = K_p\downarrow - K_p\uparrow - K_{pT}. \tag{21}$$

Dividing *equation 21* by $K_p\downarrow$

$$\phi_p = 1 - \alpha_p - \tau_p, \tag{22}$$

where ϕ_p is the PAR absorptance and τ_p is the PAR transmittance. Diurnal variation of these parameters for a cloudless and cloudy day (the same days shown in *Figure 13* for global radiation coefficients) are shown in *Figure 18*. The absorption component is considerably larger for PAR than global radiation.

Dependence of τ_p and ϕ_p on solar zenith angle was investigated. Correlation coefficients exceeded 0.82 for τ_p and 0.76 for ϕ_p on all

FIGURE 18: DIURNAL PARTITIONING OF $K_P\downarrow$

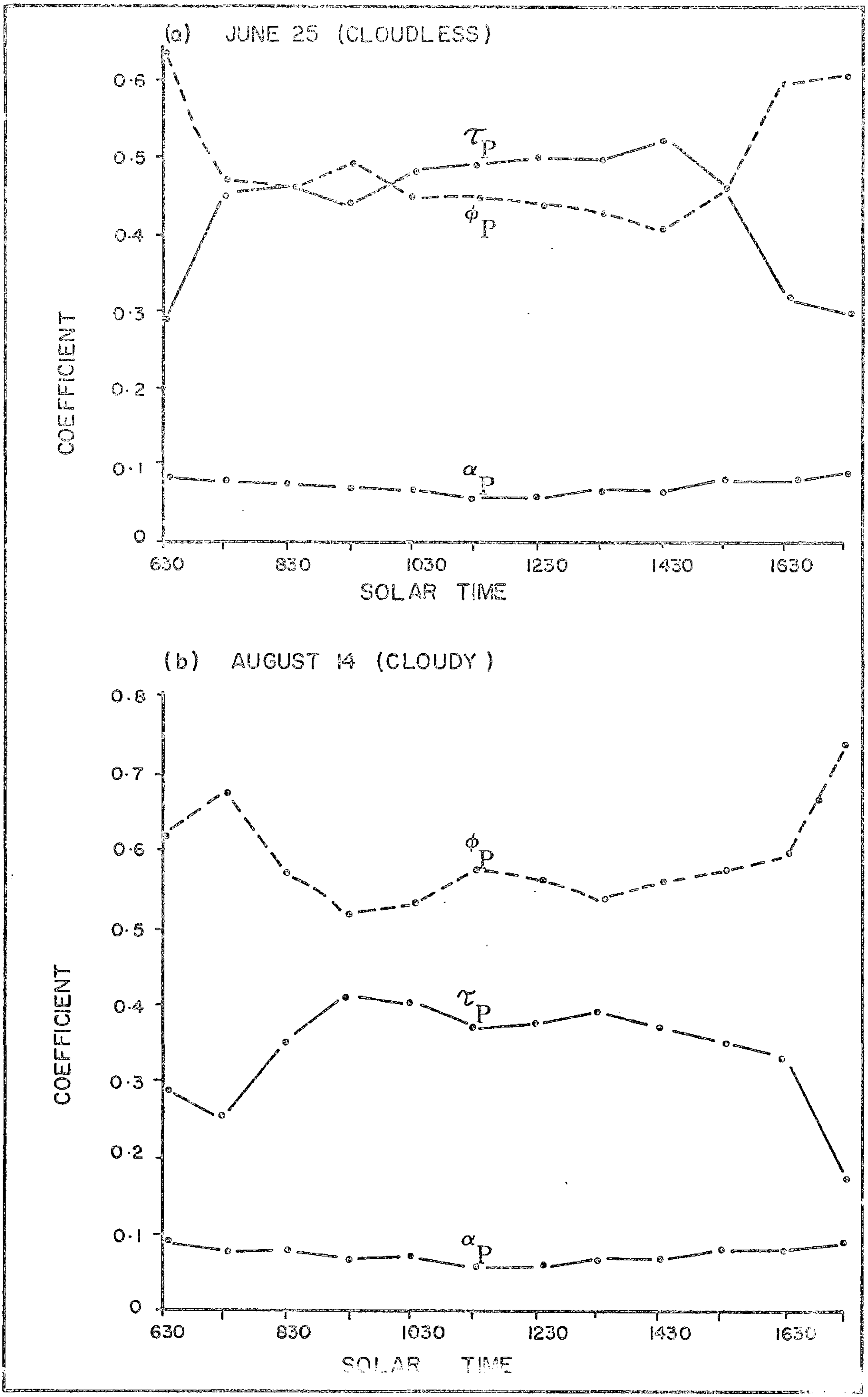

days *(Table 11)*. As with τ and $\emptyset$, diurnal variation was greatest on cloudless days as indicated by the larger regression coefficients.

Mean daily PAR coefficients are shown in *Table 12* and plotted in *Figure 19*. A seasonal trend for $\overline{\tau}_p$ and $\overline{\emptyset}_p$ is apparent, similar to that for $\overline{\tau}$ and $\overline{\emptyset}$ in *Figure 16*, with maximum $\overline{\emptyset}_p$ and minimum $\overline{\tau}_p$ in mid-August corresponding to maximum leaf development. Whereas $\overline{\tau}$ was consistently the largest component for global radiation, $\overline{\emptyset}_p$ is the largest for PAR except in the early part of the growing season. The increase of $\overline{\tau}_p$ and decline of $\overline{\emptyset}_p$ in late August is probably due to the loss of leaves during dry weather. Again, no apparent difference was observed between cloudless and cloudy days.

As an average for the entire study period, 7% of the incident PAR was reflected, 42% transmitted and 51% absorbed by the orchard.

3. Comparison of the partitioning of PAR and global radiation

By comparing the values and coefficients of the three components of global radiation and PAR from *Tables 10* and *12*, ratios of the PAR to global radiation terms were determined *(Table 13)*. Both K_{pT}/K_T and $\overline{\tau}_p/\overline{\tau}$ had largest values early in the season before full leaf development was reached. This results in a high proportion of sunflecks as indicated by high $\overline{\tau}$ values. Since sunflecks are spectrally unchanged (Looney, 1968; Monteith, 1973), τ_p and τ are identical within sunflecks; thus, high values of $\overline{\tau}_p/\overline{\tau}$ are expected early in the season. After the beginning of July, $\overline{\tau}_p/\overline{\tau}$ becomes relatively constant at 0.75, indicating only minor changes in the number of sunflecks. Unfortunately, LAI values

TABLE 11

RESULTS OF REGRESSION AND CORRELATION ANALYSIS TO SHOW THE DEPENDENCE OF τ_p AND ϕ_p ON SOLAR ZENITH ANGLE

(a = intercept, b = regression coefficient, r = correlation coefficient)

date	τ_p			ϕ_p		
	a	*b*	*r*	*a*	*b*	*r*
cloudless:						
June 11	0.82	-0.61	-0.93	0.14	0.50	0.89
June 25	0.60	-0.40	-0.83	0.34	0.32	0.80
July 9	0.53	-0.33	-0.86	0.40	0.32	0.87
July 23	0.55	-0.46	-0.94	0.40	0.41	0.92
Aug. 12	0.62	-0.65	-0.95	0.32	0.63	0.94
Aug. 15	0.56	-0.46	-0.92	0.38	0.42	0.91
Sept.4	0.59	-0.36	-0.88	0.33	0.36	0.88
cloudy:						
June 19	0.64	-0.38	-0.92	0.33	0.26	0.89
June 26	0.57	-0.23	-0.87	0.36	0.20	0.83
Aug. 7	0.44	-0.27	-0.86	0.50	0.23	0.78
Aug. 14	0.51	-0.34	-0.82	0.44	0.30	0.76
Aug. 27	0.53	-0.35	-0.90	0.43	0.28	0.83

TABLE 12

THE PARTITIONING OF $K_p\downarrow$ DAILY TOTALS

date	$K_p\downarrow$ ($Kwh\ m^{-2}$)	$K_p\uparrow$ ($Kwh\ m^{-2}$)	K_{pT} ($Kwh\ m^{-2}$)	K_{pA} ($Kwh\ m^{-2}$)	$\overline{\alpha}_p$ (assumed)	$\overline{\tau}_p$	$\overline{\phi}_p$
cloudless:							
June 11	3.67	0.25	2.21	1.21	.07	.60	.33
June 25	3.97	0.28	1.83	1.86	.07	.46	.47
July 9	3.81	0.27	1.56	1.98	.07	.41	.52
July 23	3.56	0.25	1.31	2.00	.07	.37	.56
Aug. 12	3.49	0.25	1.18	2.06	.07	.34	.59
Aug. 15	2.78	0.20	1.05	1.53	.07	.38	.55
Sept.4	2.28	0.17	0.96	1.15	.07	.42	.51
mean					.07	.43	.50
cloudy:							
June 19	2.56	0.18	1.31	1.07	.07	.51	.42
June 26	2.26	0.17	1.13	0.96	.07	.50	.43
Aug. 7	2.34	0.17	0.78	1.39	.07	.33	.60
Aug. 14	1.71	0.12	0.61	0.98	.07	.36	.57
Aug. 27	1.35	0.10	0.48	0.97	.07	.36	.57
mean					.07	.41	.52
mean all days					.07	.42	.51

FIGURE 19: SEASONAL VARIATION OF THE PAR REFLECTION, TRANSMISSION AND ABSORPTION COEFFICIENTS

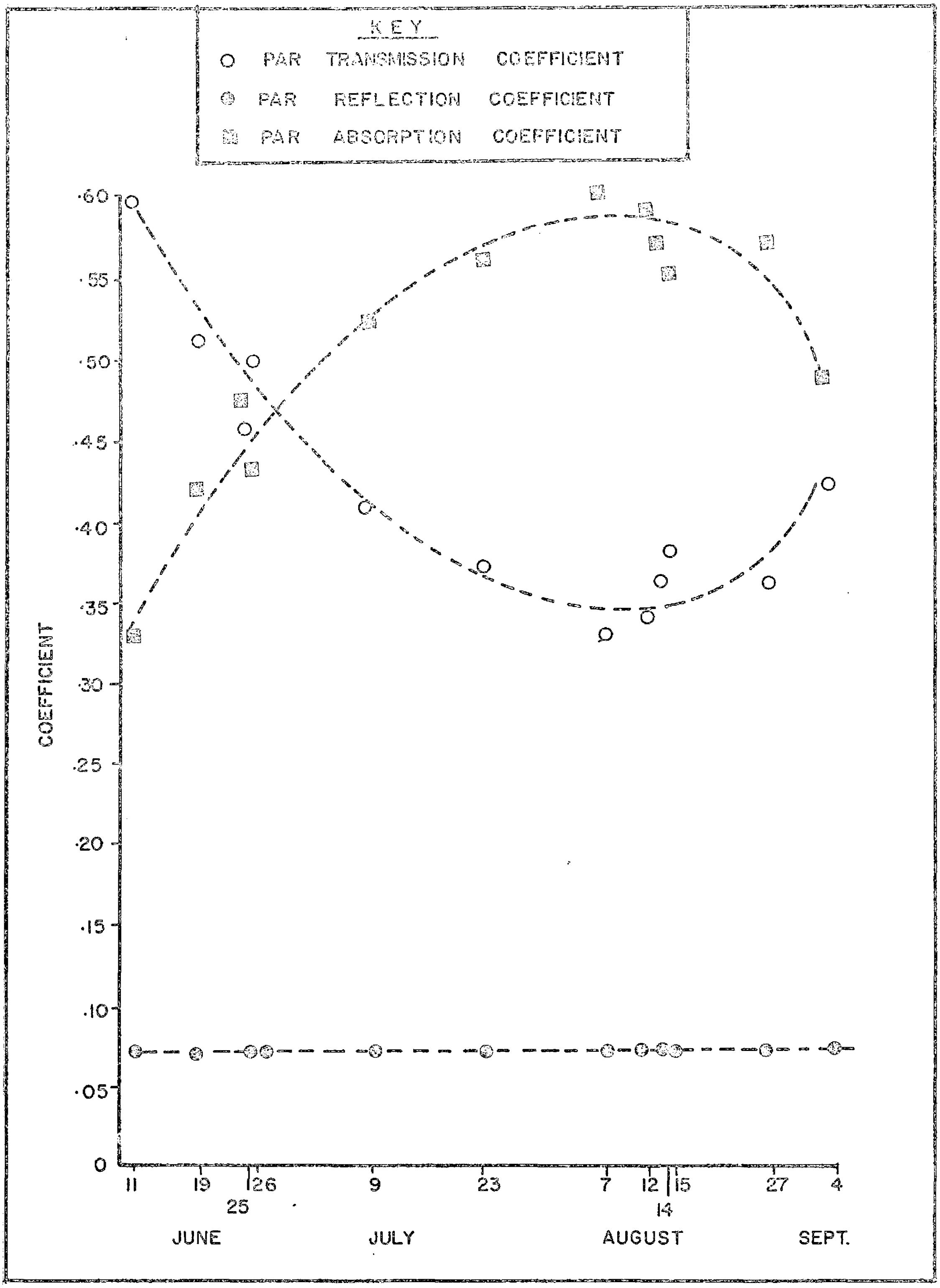

TABLE 13

RATIOS OF DAILY TOTALS OF PAR TERMS TO GLOBAL RADIATION TERMS

date	$K_p\downarrow/K\downarrow$	$K_p\uparrow/K\uparrow$	$\overline{\alpha}_p/\overline{\alpha}$	K_{pT}/K_T	$\overline{\tau}_p/\overline{\tau}$	K_{pA}/K_A	$\overline{\emptyset}_p/\overline{\emptyset}$
June 11	0.49	0.19	0.39	0.44	0.90	1.07	2.20
June 19	0.49	0.18	0.37	0.42	0.85	0.97	2.00
June 25	0.49	0.19	0.39	0.39	0.79	0.96	1.96
June 26	0.49	0.19	0.37	0.42	0.86	0.92	1.87
July 9	0.49	0.19	0.39	0.38	0.77	0.88	1.79
July 23	0.49	0.19	0.39	0.36	0.74	0.86	1.75
Aug. 7	0.49	0.18	0.37	0.36	0.72	0.84	1.71
Aug. 12	0.49	0.19	0.39	0.37	0.76	0.78	1.59
Aug. 14	0.49	0.18	0.37	0.36	0.73	0.87	1.78
Aug. 15	0.49	0.20	0.39	0.36	0.75	0.87	1.77
Aug. 27	0.49	0.19	0.37	0.36	0.75	0.85	1.73
Sept.4	0.49	0.21	0.41	0.38	0.76	0.87	1.82
mean	0.49	0.19	0.38	0.38	0.79	0.90	1.79
mean (excluding June)		0.19	0.38	0.37	0.75	0.85	1.73

through the season were not available to substantiate this.

It has earlier been shown that $K_p\downarrow$ can be predicted from $K\downarrow$. In order to establish a similar relationship for the transmitted component, regression analysis *(Figure 20)* was used indicating

$$\bar{\tau}_p = -0.25 + 1.25\,\bar{\tau}, \quad r = 0.985. \tag{23}$$

This shows that $\bar{\tau}_p$ is a function of $\bar{\tau}$ within the limits from which the relationship was derived (i.e. $0.45 < \bar{\tau} < 0.70$). For $\bar{\tau} = 1$, the relationship is also valid; however, extension of the relationship to values with $\bar{\tau}$ less than 0.45 can result in negative $\bar{\tau}_p$ values. Using logarithmic values did not improve the relationship for the range of data available.

Since $\bar{\tau}$ is dependent on plant density and development, *equation 23* indicates that PAR is attenuated more rapidly than global radiation as plant density increases. This has been observed by Szeicz (1970) and Rodskjer (1971).

Application of *equation 23* to hourly values on individual days *(Table 14)* showed over- and under-estimation of up to 35%. The relationship is therefore limited to daily estimates of the PAR transmission coefficient.

Therefore, for this orchard, incident PAR and its components can be estimated on a daily basis entirely from knowledge of incident global radiation relationships; that is $K_p\downarrow$ from *equation 19*, $K_p\uparrow$ from knowledge of spectral reflectance, K_{pT} from $\bar{\tau}_p$ in *equation 23*, and K_{pA} as a residual *(equation 21)*.

FIGURE 20: RELATIONSHIP BETWEEN PAR AND GLOBAL RADIATION TRANSMISSION COEFFICIENTS

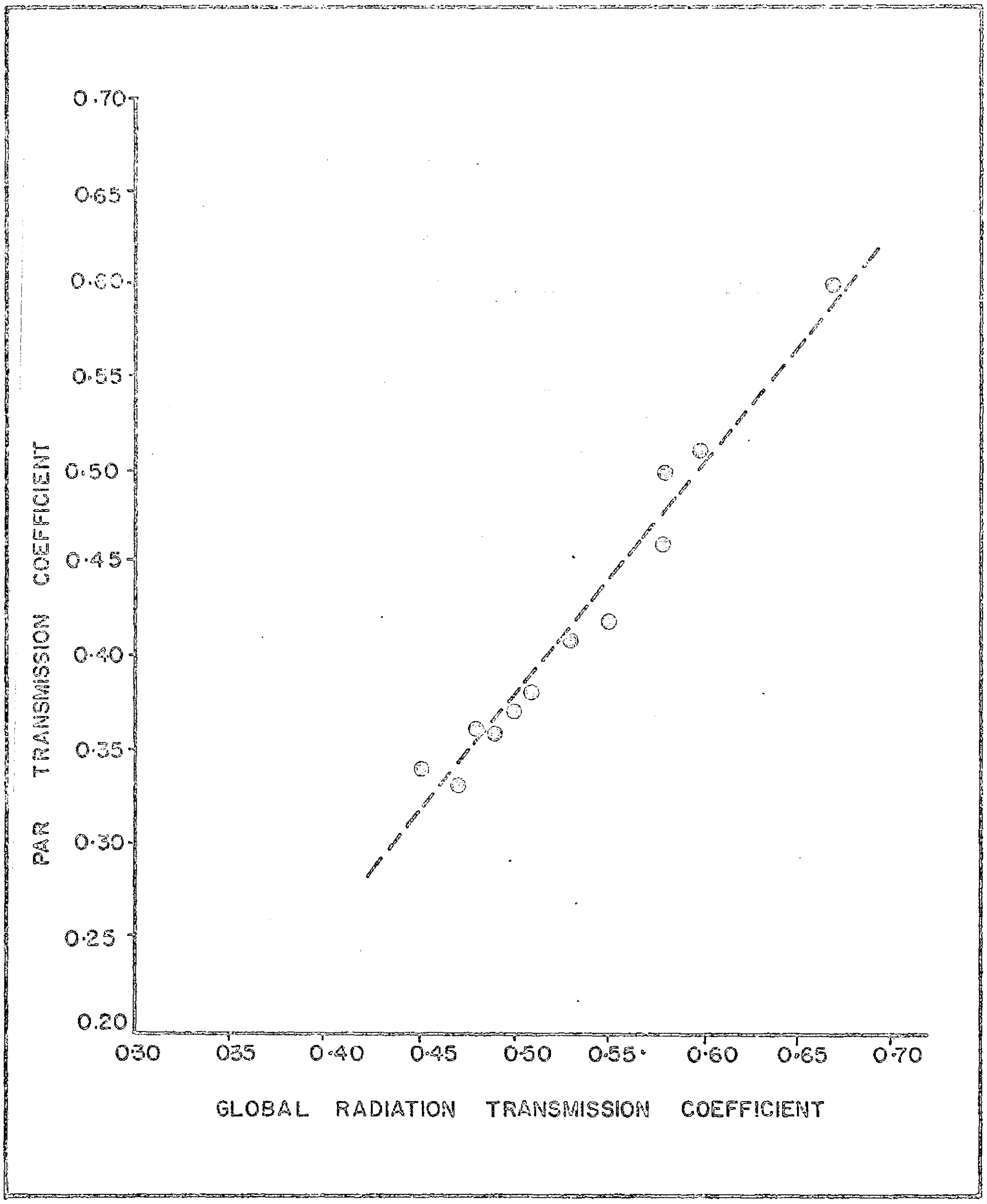

TABLE 14

APPLICATION OF *EQUATION 23* TO HOURLY VALUES

June 25

LAT	τ	τ_p(calc)	τ_p(meas)	$\Delta\tau_p$	%difference
0630	.45	.31	.28	+.03	10%
0730	.57	.46	.45	+.01	2%
0830	.57	.46	.46	0	0%
0930	.57	.46	.44	+.02	4%
1030	.61	.51	.48	+.03	6%
1130	.65	.56	.49	+.07	13%
1230	.64	.55	.50	+.05	10%
1330	.60	.50	.50	0	0%
1430	.62	.53	.52	+.01	2%
1530	.52	.33	.46	-.13	-33%
1630	.43	.29	.32	-.03	-10%
1730	.43	.29	.30	-.01	-3%

August 14

LAT	τ	τ_p(calc)	τ_p(meas)	$\Delta\tau_p$	%difference
0630	.44	.30	.29	+.01	3%
0730	.36	.20	.25	-.05	-33%
0830	.48	.35	.35	0	0%
0930	.49	.36	.41	-.05	-13%
1030	.49	.36	.40	-.04	-11%
1130	.48	.35	.37	-.02	-6%
1230	.49	.36	.38	-.02	-6%
1330	.48	.35	.39	-.04	-11%
1430	.48	.35	.37	-.02	-6%
1530	.47	.34	.35	-.01	-3%
1630	.44	.30	.33	-.03	-9%
1730	.33	.24	.17	+.07	35%

CHAPTER VI

PROBLEM OF USING MEAN TRANSMISSIONS

1. Use of the mean

In the preceeding chapters, transmitted radiation was determined using means of measurements from a traversing sensor. Examples of transmitted radiation obtained by strip-chart recorder are shown for a cloudless and a cloudy traverse in *Figure 21*. The curves join the original data points on the chart record. The magnitude and frequency of variation are both less for the cloudy traverse. Frequency distributions *(Figure 22)* show that although the mean may be representative under cloud, it is inappropriate for cloudless conditions. The mean is amongst the least frequently measured values in the bimodal distribution. This distribution results from the high incidence of sunflecks. The position of sunflecks changes with solar zenith and azimuth angles. Hence, their influence may be evenly spread over the ground surface. Frequency distributions of transmitted energy using all the data for the two days were calculated *(Figure 23)*. Low value data from 0630 and 1730 traverses were not used. For cloudy days, the distribution is nearly normal. On cloudless days, the distribution is skewed indicating that the influence of sunflecks is not evenly distributed.

2. The case for two transmission regimes

The frequency distribution for cloudless data *(Figure 22a)*

FIGURE 21: TRANSMITTED RADIATION FROM A MOVING SENSOR TRAVERSE

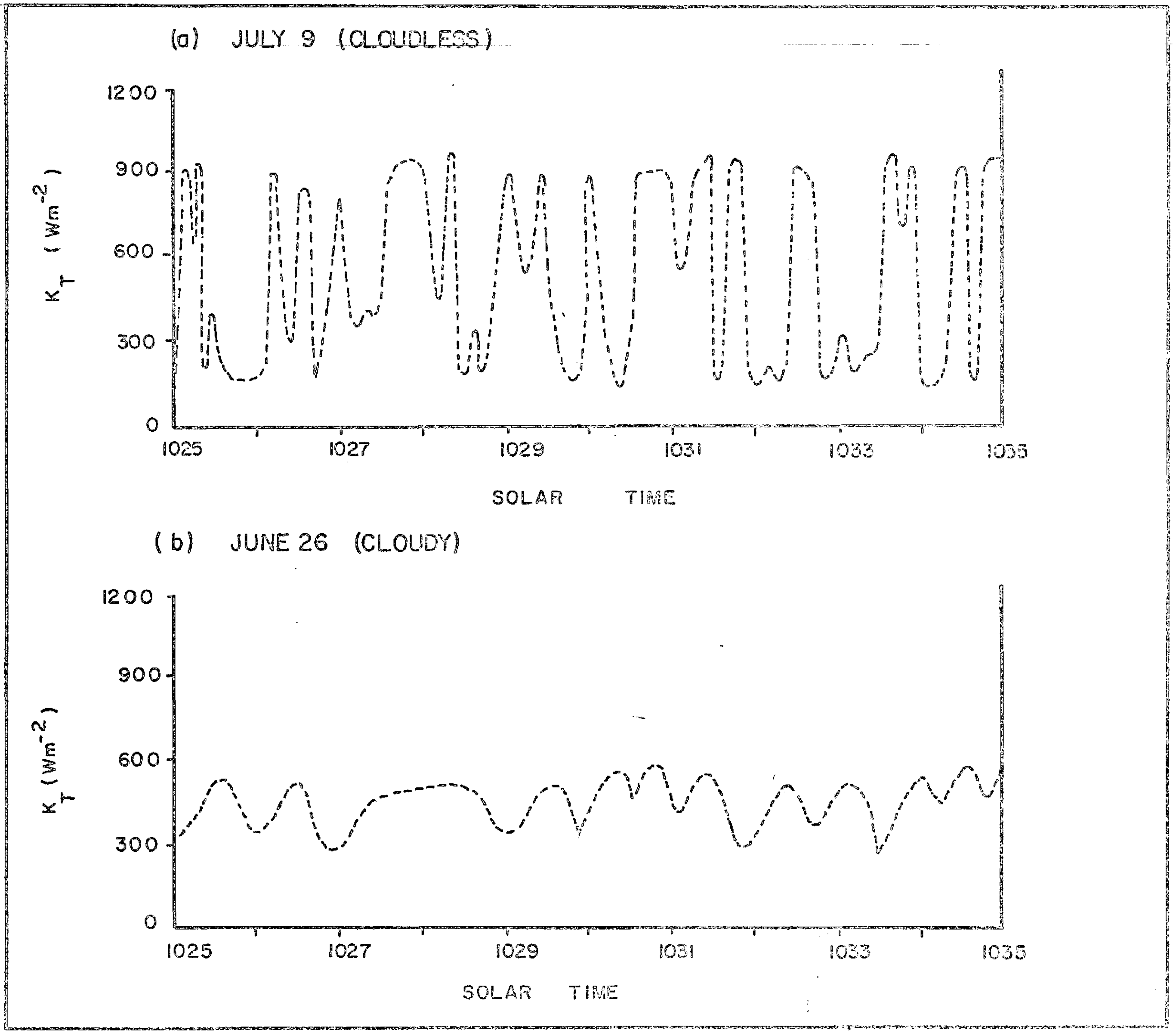

FIGURE 22: K_T FREQUENCY DISTRIBUTION HISTOGRAMS FOR A SINGLE TRAVERSE

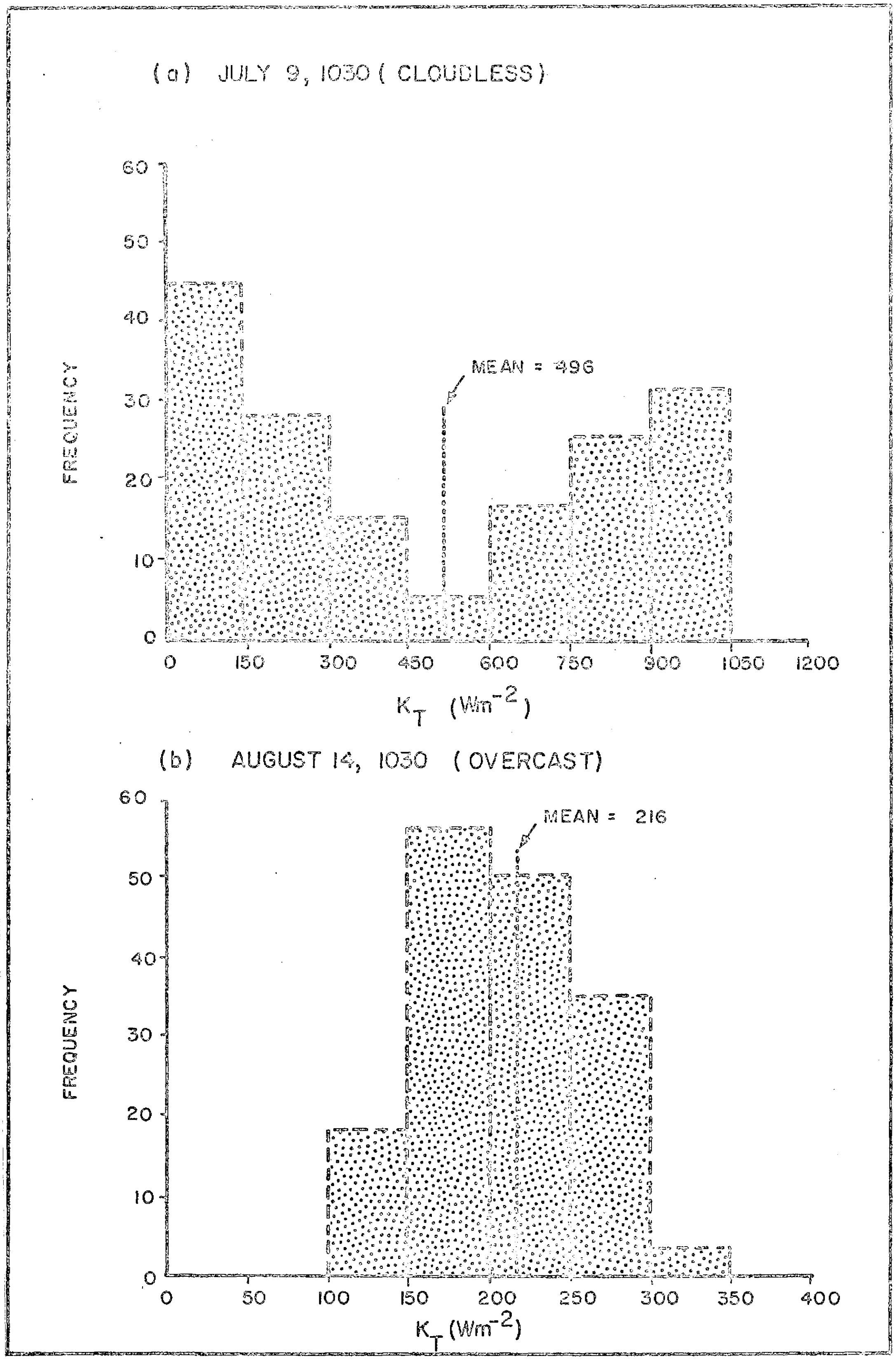

FIGURE 23: K_T FREQUENCY DISTRIBUTION HISTOGRAMS FOR COMPLETE DAYS

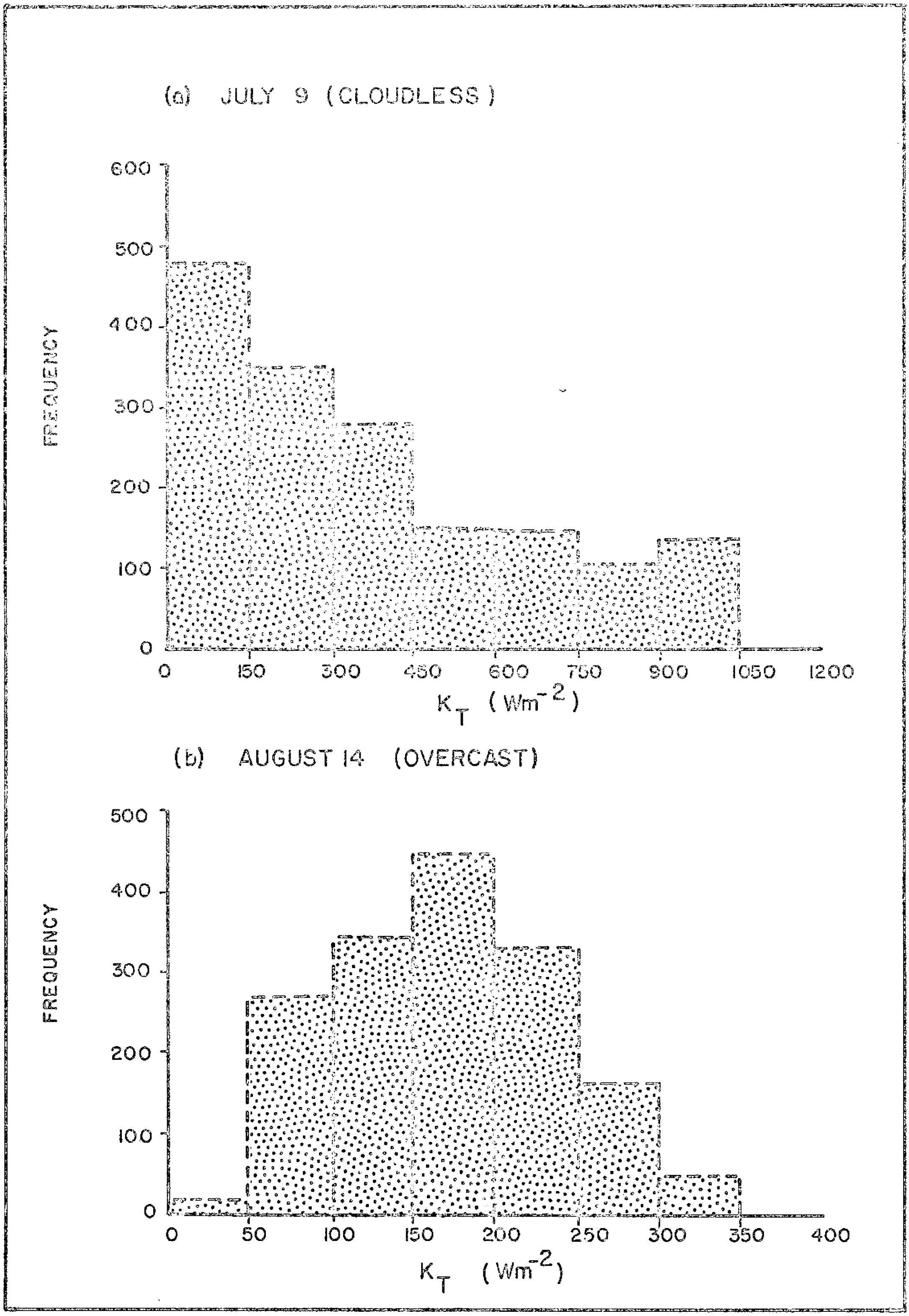

suggests two distinct transmitted radiation regimes. Difficulty exists in defining the limits of the two regimes especially early and late in the day. In general, a 'low energy regime' was considered to be all the classes in the frequency distribution before the least frequently occurring class in the bimodal distribution. Values of transmitted global radiation for the 'low energy regime' were calculated for July *(Table 15)*. Low energy regime transmission coefficients $\tau(L)$ exhibited no systematic diurnal trend. Summed for the entire day, $\overline{\tau}(L) = 0.26$, about half the value for $\overline{\tau}$.

To determine illumination of the lower canopy, measurements beneath individual trees to avoid large sunflecks are required. Transmission of energy through a tree is predominately of the low energy type. However, some energy would be available to lower branches in small sunflecks. Measurement of this energy would require additional sensing of transmitted radiation at different levels within the foliage of a single tree. Therefore, additional field work is needed to adequately measure transmitted radiation on cloudless days.

TABLE 15

LOW ENERGY REGIME TRANSMISSION COEFFICIENTS FOR JULY 9

LAT	$K\downarrow$ (Wm^{-2})	K_T (Wm^{-2})	τ	$K_T(L)$ (Wm^{-2})	$\tau(L)$
0630	244	98	.40	75	.31
0730	454	209	.43	125	.28
0830	642	335	.52	190	.30
0930	810	440	.54	250	.31
1030	900	496	.55	193	.21
1130	949	593	.63	265	.28
1230	942	579	.62	238	.25
1330	726	391	.54	222	.31
1430	656	307	.47	128	.20
1530	621	293	.47	138	.22
1630	475	202	.43	125	.26
1730	251	91	.36	75	.30
Daily totals	7.78 ($Kwh\ m^{-2}$)	4.12 ($Kwh\ m^{-2}$)	$\bar{\tau} = .53$	2.01 ($Kwh\ m^{-2}$)	$\bar{\tau}(L) = .26$

CHAPTER VII

CONCLUSIONS

In accordance with the main objectives of the study, there are two sets of conclusions.

1. The radiation balance components at the upper surface of a dwarf apple orchard are similar to those for a single tree in an earlier investigation. Incoming global radiation on cloudless days agreed well with theoretical determinations from Houghton's (1954) model while Swinbank's (1963) model tended to over-estimate daytime incoming longwave radiation. Incoming diffuse radiation ratios indicated a possible pollution effect associated with lake breezes.

The reflection coefficient of the orchard was slightly higher than for a single tree and was also higher on cloudy than cloudless days. Dependence on solar zenith angle was evident, confirming results for various crops. No seasonal trend was evident.

Linear regression analysis showed high correlations between net and net global radiation indicating that net radiation could be estimated from a measure of net global radiation. Heating coefficients showed considerable variation and no seasonal pattern. Differences between the mean heating coefficient of this orchard and those from studies on another orchard and a single tree resulted in only 2 to 3% and 7 to 12% difference in net radiation determinations. Similar analysis for Gay's longwave exchange coefficient showed that differences between the mean coefficient for the orchard and single tree produced significant differences in net longwave radiation estimations.

2. The use of a moving sensor rather than stationary sensors has the advantage of low cost and good spatial coverage. Coefficients for the partitioning of incident global radiation were calculated for hourly and daily periods. Some dependence on solar zenith angle was found for all three coefficients. Seasonal variation in mean daily transmission and absorption corresponded to leaf development with minimum transmission and maximum absorption in mid-August. Transmission was consistently the largest component while reflection was the smallest. Averaged for the entire study period, 18% of incident global radiation was reflected, 53% transmitted and 29% absorbed by the trees.

Incident PAR was 49% of the global radiation. Transmission and absorption coefficients showed similar zenith angle dependence and seasonal variation to global radiation coefficients. Mean daily PAR absorption coefficients were the largest component for most of the season and reflection was again smallest. Averaged for the entire study period, 7% of incident PAR was reflected, 42% transmitted and 51% absorbed by the canopy.

Global radiation and PAR transmission coefficients were related linearly. A lower limit of global radiation transmission exists beyond which the relationship does not hold. For this orchard, PAR components of incident radiation can be calculated entirely from knowledge of the global radiation components.

Further study is needed to estimate incoming radiative fluxes under cloudy skies and to adequately evaluate $L\downarrow$ for cloudless skies. The validity and limits of the PAR and global radiation transmission coefficient relationship warrants investigation. Use of mean transmissions for considering transmitted radiation available to illuminate the lower canopy is valid only on cloudy days. For cloudless days, there are two transmission regimes, one for trees and one for inter-tree space. The spatial and temporal limits of these two regimes are difficult to define. Measurements beneath the individual trees and at different levels within the trees should yield information on the radiation available to the lower canopy.

REFERENCES

Anderson, M.C., 1966: Some problems of simple characterization of the light climate in plant communities, in *Light as an Ecological Factor*, ed. R. Bainbridge, G.C. Evans and O. Rackham, Blackwell Scientific Publications, Oxford, 77-90.

_______________, 1969: A comparison of two theories of scattering of radiation in crops, *Agric. Meteor.*, 6, 399-405.

Bray, J.R., J.E. Sanger and A.L. Archer, 1966: The visible albedo of surfaces in central Minnesota, *Ecol.*, 47, 524-531.

Brown, G.W., 1973: Measuring transmitted global radiation with fixed and moving sensors, *Agric. Meteor.*, 11, 115-121.

Chang, Jen-Hu, 1968: *Climate and Agriculture - An Ecological Survey*, Aldine, Chicago, 304 p.

Coulson, K.L. and D.W. Reynolds, 1971: The spectral reflectance of natural surfaces, *J. Appl. Meteor.*, 10, 1285-1295.

Davies, J.A., 1967: A note on the relationship between net radiation and solar radiation, *Quart. J.R. Meteor. Soc.*, 93, 109-115.

Davies, J.A. and P.H. Buttimor, 1969: Reflection coefficients, heating coefficients and net radiation at Simcoe, southern Ontario, *Agric. Meteor.*, 6, 373-386.

Davies, J.A., P.J. Robinson and M. Nunez, 1970: *Radiation Measurement over Lake Ontario and the Determination of Emissivity*, First report, Contract No.H081276, Gov. Canada, Dept. Environment, Canada Centre for Inland Waters, Burlington, 85 p.

Drummond, A.J., 1956: On the measurement of sky radiation, *Arch. Meteor. Geophys. Bioklim. (B)*, 7, 413-436.

Efimova, N.A., 1971: Geographical distribution of the sums of photosynthetically active radiation, *Soviet Geog.*, 12, 66-74.

Fritschen, L.J., 1967: Net and solar radiation relations over irrigated field crops, *Agric. Meteor.*, 4, 55-62.

Gates, D.M., 1965: Energy, plants and ecology, *Ecol.*, 46, 1-13.

Gay, L.W., 1971: The regression of net radiation upon solar radiation, *Arch. Meteor. Geophys. Bioklim. (B)*, 19, 1-14.

Houghton, H.G., 1954: On the annual heat balance of the northern hemisphere, *J. Meteor.*, 11, 1-9.

Idso, S.B., D.G. Baker and B.L. Blad, 1969: Relations of radiation fluxes over natural surfaces, *Quart. J.R. Meteor. Soc.*, 95, 244-257.

Impens, I.I. and R. Lemeur, 1969a: The radiation balance of several field crops, *Arch. Meteor. Geophys. Bioklim. (B)*, 17, 261-268.

__________ and __________, 1969b: Extinction of net radiation in different crop canopies, *Arch. Meteor. Geophys. Bioklim. (B)*, 17, 403-412.

Kalma, J.D. and R. Badham, 1972: The radiation balance of a tropical pasture, I. The reflection of short-wave radiation, *Agric. Meteor.*, 10, 251-259.

Kalma, J.D. and G. Stanhill, 1969: The radiation climate of an irrigated orange plantation, *Solar Energy*, 12, 491-508.

Kyle, W.J., 1971: *Daytime Radiation Regimes Within a Corn Canopy*, Publications in climatology No.2, McMaster University, Dept. of Geography, Hamilton, Ontario, 140 p.

Landsberg, J.J., D.B.B. Powell and D.R. Butler, 1973: Microclimate in an apple orchard, *J. Appl. Ecol.*, 10, 881-896.

Latimer, J.R., 1972: *Radiation Measurement*, International Field Year for the Great Lakes, Technical manual series, No.2, 53 p.

Looney, N.E., 1968: Light regimes within standard size apple trees as determined spectrophotometrically, *Proc. Amer. Soc. Hort. Sci.*, 93, 1-6.

Monteith, J.L., 1959: The reflection of short-wave radiation by vegetation, *Quart. J.R. Meteor. Soc.*, 85, 386-392.

__________, 1965: Radiation and crops, *Exp. Agric.*, 1, 241-251.

__________, 1973: *Principles of Environmental Physics*, Edward Arnold (Publishers) Ltd., London, 241 p.

Monteith, J.L. and G. Szeicz, 1961: The radiation balance of bare soil and vegetation, *Quart. J.R. Meteor. Soc.*, 87, 159-170.

Mukammal, E.I., 1965: Ozone as a cause of tobacco injury, *Agric. Meteor.*, 2, 145-165.

____________, 1971: Some aspects of radiant energy in a pine forest, *Arch. Meteor. Geophys. Bioklim. (B)*, 19, 29-52.

Myers, V.I. and W.A. Allen, 1968: Electrooptical remote sensing methods as nondestructive testing and measuring techniques in agriculture, *Appl. Optics*, 7, 1819-1838.

Nkemdirim, L.C., 1973: Radiative flux relations over crops, *Agric. Meteor.*, 11, 229-242.

Nunez, M., J.A. Davies and P.J. Robinson, 1971: *Solar Radiation and Albedo at a Lake Ontario Tower Site*, Third report, Contract No. H081276, Gov. Canada, Dept. Environment, Canada Centre for Inland Waters, Burlington, 82 p.

Paltridge, G.W., 1970a: Day-time long-wave radiation from the sky, *Quart. J.R. Meteor. Soc.*, 96, 645-653.

____________, 1970b: A filter for absorbing photosynthetically-active radiation and examples of its use, *Agric. Meteor.*, 7, 167-174.

Proctor, J.T.A., W.J. Kyle and J.A. Davies, 1972: The radiation balance of an apple tree, *Can. J. Bot.*, 50, 1731-1740.

Rehder, A., 1962: *Manual of Cultivated Trees and Shrubs*, Second edition, 996 p.

Reifsnyder, W.E., G.M. Furnival and J.L. Horowitz, 1971: Spatial and temporal distribution of solar radiation beneath forest canopies, *Agric. Meteor.*, 9, 21-37.

Robinson, P.J., J.A. Davies and M. Nunez, 1972: *Longwave Radiation Exchanges over Lake Ontario*, Fourth report, Contract No. H081276, Gov. Canada, Dept. Environment, Canada Centre for Inland Waters, Burlington, 135 p.

Rodskjer, N., 1971: A pyranometer with dome RG8 for use in plant communities, *Arch. Meteor. Geophys. Bioklim. (B)*, 19, 307-320.

Rodskjer, N. and A. Kornher, 1971: Uber die bestimming der strahlungsenergie im wellenlangenbereich von 0.3-0.7 μ in Pflanzenbestanden, *Agric. Meteor.*, 8, 139-150.

Schomaker, C.E., 1968: Solar radiation measurements under a spruce and a birch canopy during May and June, *Forest Sci.*, 14, 31-38.

Sellers, W.D., 1965: *Physical Climatology*, U. of Chicago Press, Chicago, 272 p.

Stanhill, G., 1970: Some results of helicopter measurements of the albedo of different land surfaces, *Solar Energy*, 13, 59-66.

Stanhill, G., G.J. Hofstede and J.D. Kalma, 1966: Radiation balance of natural and agricultural vegetation, *Quart. J.R. Meteor. Soc.*, 92. 128-140.

Swinbank, W.C., 1963: Longwave radiation from clear skies, *Quart. J.R. Meteor. Soc.*, 89, 339-348.

Szeicz, G., 1966: Field measurements of energy in the 0.4-0.7 micron range, in *Light as an Ecological Factor*, ed. R. Bainbridge, G.C. Evans and O. Rackham, Blackwell Scientific Publications, Oxford, 41-52.

Szeicz, G., 1970: *Spectral Composition of Solar Radiation and its Penetration in Crop Canopies*, Ph.D. Thesis, University of Reading, England.

Tajchman, S.J., 1972: The radiation and energy balances of coniferous and deciduous forests, *J. Appl. Ecol.*, 9, 359-377.

Vézina, P.E. and M.M. Grandtner, 1965: Phenological observations of spring geophytes in Quebec, *Ecol.*, 46, 869-872.

Yocum, C.S., L.H. Allen and E.R. Lemon, 1964: Photosynthesis under field conditions VI. Solar radiation balance and photosynthetic efficiency, *Agron. J.*, 56, 249-253.